On Moment Capacity and Flexural Ductility in Doubly Symmetric Web-Tapered I-Girders

B.S. MILLER and C.J. EARLS

Web-tapered I-girder cross-sections are frequently employed within the primary framing system of metal buildings. The web-tapered members are used within gabled bents that serve as a primary lateral and gravity load resisting system within a given building. While bracing members are frequently employed to control instabilities in the direction normal to the tapered gable bents, the bents themselves resist in-plane lateral loads as rigid frames through the development of significant internal moments. As a result of the moment connections between columns and rafters in these frames, gravity loads also tend to produce significant flexural demands on the entire primary framing system; both rafters and columns.

Interestingly enough, despite the detailed experimental and analytical studies carried out by earlier researchers (Lee, Morrell, and Ketter, 1972; Morrell and Lee, 1974), significant confusion still exists as to the flexural capacity and ductility of doubly symmetric web-tapered I-girder members. Specifically, it has been suggested that web-tapered members ought to be considered capable of developing their full plastic cross-sectional capacity at any given position along the member longitudinal axis, so long as compactness and bracing requirements are sufficient to exclude the possibility of significant erosion in ultimate capacity due to local and/or lateral-torsional buckling (Lee, Ketter, and Hsu, 1981). The AISC *Load and Resistance Factor Design Specification for Structural Steel Buildings* (AISC, 1999), hereafter referred to as the AISC LRFD Specification, might be thought to have adopted a similar position to the foregoing since Appendix F of that document contains a statement to the effect that the web-tapered member provisions contained in that Appendix are meant to augment the more general provisions provided in the main body of the specification (see Appendix F, Section F3). Appendix F provides design formulae strictly addressing the limit state of lateral-torsional buckling (Appendix F, Section F3.4). Thus one might conclude that it is reasonable to assume that the yielding limit state of Chapter F (Section F1.1), based on the development of the full plastic capacity, is a valid limit state to expect from properly proportioned web-tapered I-shaped beams. Proper proportioning would mean that the bracing requirements called out in Chapter F (Sections F1.2a(a) and F1.3), in addition to the cross-sectional compactness criteria from Chapter B (Table B5.1), are satisfied. The confusion, alluded to earlier, arises since the introductory paragraph in Chapter F clearly excludes web-tapered members when it states that "this chapter applies to compact and noncompact prismatic members…" The net effect of this exclusionary wording is that the AISC LRFD Specification limits the capacity of web-tapered members to be no greater than the moment to cause first yield in any fiber in a tapered cross-section located at any position along the longitudinal axis of the member. This contradicts the recommendations of Lee and others (1981) and so the present research is partly aimed at exploring the validity in assuming web-tapered beams to be capable of developing their full plastic capacity. The present research also explores requirements for cross-sectional compactness in these same members.

BASIS FOR AISC LRFD WEB-TAPERED FLEXURAL PROVISIONS

The goal of the AISC compactness criteria promulgated in Table B5.1 of the AISC LRFD Specification (AISC, 1999) is to identify plate slenderness limits, λ_p, for cross-sectional plate components such that satisfaction of said limits will result in an overall flexural cross-section able to accommodate sufficient plastic hinge rotation to support system-wide moment redistribution, as required for the development of a collapse mechanism. While web-tapered I-shaped cross-sections are not specifically treated in this table, the assumption is that the compactness criteria applying to prismatic

B.S. Miller is research assistant, department of civil & environmental engineering, University of Pittsburgh, Pittsburgh, PA.

C.J. Earls is associate professor & William Kepler Whiteford Faculty Fellow, department of civil & environmental engineering, University of Pittsburgh, Pittsburgh, PA.

I-shaped members should be extendable to web-tapered members having moderate tapers [in other words, 15° of taper or less (Lee and others, 1972)]. This notion of portability in prismatic member provisions to the case of web-tapered I-shaped members of moderate taper is based on findings from earlier research (Boley, 1963) indicating that standard flexural theory, based on prismatic member assumptions, are extendable to the case of beams with gentle web tapers. This earlier research finding has been used as a basis for extrapolating prismatic member design equations to moderately tapered I-shaped members.

The research of Lee and co-workers (Lee and others, 1972 and 1981; Morrell and Lee, 1974) led directly to web-tapered member flexural provisions that are in Appendix F of the AISC LRFD Specification (1999). Since the earlier research of Lee and co-workers focused only on web-tapered I-shaped cross-sections possessing double symmetry, constant web thickness, and web tapers of 15° or less, these restrictions have been adopted in the AISC LRFD Appendix F (Appendix F, Section F3.1) provisions. As indicated earlier, the Appendix F flexural provisions address the limit state of lateral-torsional buckling in the form of Equation A-F3-3, reproduced below as Equation 1:

$$M_n = \left(\frac{5}{3}\right) S_x' F_{b\gamma} \tag{1}$$

where

S_x' = the section modulus in the critical section of the unbraced beam length under consideration.

$F_{b\gamma}$ is given by AISC LRFD Equation A-F3-4 and shown below as Equation 2:

$$F_{b\gamma} = \frac{2}{3}\left[1.0 - \frac{F_y}{6B\sqrt{F_{s\gamma}^2 + F_{w\gamma}^2}}\right] F_y \le 0.60F_y \tag{2}$$

Equation 2 is an inelastic transition relationship spanning the region of web-tapered proportions where inelastic lateral-torsional buckling governs. The relationship in Equation 2 is loosely based on the CRC (Column Research Council—now SSRC) Basic Column Curve. In the case where $F_{b\gamma}$ is less than or equal to $F_y/3$ (in other words, when the critical lateral-torsional buckling stress is less than $\frac{2}{3}(F_y/2)$; 0.6 times the maximum residual stress magnitude, then Equation 3 governs:

$$F_{b\gamma} = B\sqrt{F_{s\gamma}^2 + F_{w\gamma}^2} \tag{3}$$

In all of the foregoing, the following expressions for critical lateral-torsional buckling stress hold:

$$F_{s\gamma} = \frac{0.41E}{(h_s L d_o / A_f)} \tag{4}$$

$$F_{w\gamma} = \frac{5.9E}{(h_w L / r_{To})^2} \tag{5}$$

Equations 4 and 5 are essentially slightly modified versions of the AISC *Specification for Structural Steel Buildings—Allowable Stress Design & Plastic Design* (AISC, 1989), hereafter referred to as the AISC ASD Specification, equations for prismatic member elastic lateral-torsional buckling for the cases where either St. Venant's torsion (Equation 4), or warping/non-uniform torsion (Equation 5) dominate the form of the internal resisting moment within the beam. Equations 4 and 5 deviate from the corresponding AISC ASD Specification formulation only by the presence of the *h*-terms in the denominators of Equations 4 and 5. These length modification terms arise out of the philosophical approach taken by Lee and his co-workers (Lee and others, 1972): "Theoretical solutions are first obtained, then, using these solutions, the AISC prismatic member design formulas are modified to effect the same solutions by the introduction of appropriate multiplying factors which are dependent only on the tapering geometry." The theoretical solutions used by Lee and his co-workers emanated from an approximate solution to the variational statement of the web-tapered beam lateral-torsional buckling problem. Lee and others formulated internal strain energies and external loading potentials using an approach consistent with that of Bleich (1952), but modified for the tapered member geometry. The total potential for the system was then stated directly so that the stationary condition could be found using the calculus of variations. The resulting weak form statement of equilibrium was retained by Lee and others and solved approximately using trial functions and the Rayleigh-Ritz Method. While it would be possible to convert the weak form statement into a strong form, differential equation based statement of the equilibrium condition, the solution of the subsequent boundary value problem would be somewhat cumbersome due to the statistical quality of the natural boundary conditions that would be required in such an approach. In the integral form of the weak statement used by Lee and others (1972), consideration of kinematical boundary conditions is all that is required as part of the trial function selection process since the natural (or force) boundary conditions are implied in the integral equations.

A standard bifurcation approach was subsequently undertaken to identify the critical stress for the given beam in the lateral-torsional mode. Lee and others (1972) then took the approach that this capacity could be related to existing AISC

ASD Specification prismatic member capacities through an approach encapsulated by the statement:

$$\frac{Rayleigh-Ritz\_Derived\_Tapered\_Member\_Capacity}{AISC\_Prismatic\_Member\_Strength\_Based\_On\_Smaller\_End} = f(\gamma, d_o, b, t_f, t_w, L)$$

The function on the right hand side of the foregoing equation represents the h values appearing in the denominators of Equations 4 and 5. Consideration of five representative cross-sections for use in the smaller end of web-tapered members commonly encountered in practice resulted in theoretical solutions that could be used with curve fitting techniques to arrive at the following expressions for h_s and h_w, as outlined in Appendix F, Section F3.4 of the AISC LRFD Specification:

$$h_s = 1.0 + 0.23\gamma\sqrt{Ld_o/A_f} \quad (6)$$

$$h_w = 1.0 + 0.00385\gamma\sqrt{L/r_{To}} \quad (7)$$

where

L = unbraced length
A_f = area of the compression flange
d_o = cross-sectional depth at the smaller end of the web-tapered beam
r_{To} = radius of gyration at the smaller end, considering only the compression flange plus one-third of the compression web area, taken about an axis in the plane of the web.

In Equations 2 and 3, the beneficial effects of the end-restraint afforded to the critical unbraced length through continuity with adjacent spans, as well as the strength increase associated with the inevitable moment gradient present in such a case, is accounted for in the *B*-term defined in Equations A-F3-8 through A-F3-11 in Appendix F of the AISC LRFD Specification. This continuity term was adopted into the AISC LRFD Specification Appendix F provisions based on the research of Morrell and Lee (1974). Morrell and Lee studied the beneficial effects of adjacent-span continuity and moment gradient on the critical buckling stress of web-tapered beams using a finite element approach wherein the web-tapered cross-section was modeled as a stepped beam through the use of a mesh of multiple prismatic beam finite elements assembled so as to emulate the effects of actual cross-sectional taper in a piece-wise fashion. Representative web-tapered cross-sectional proportions, as well as four different unbraced lengths, were considered in addition to five different taper ratios and five different moment gradients (ranging from single to double curvature). Morrell and Lee then employ a standard linearized eigenvalue buckling approach to obtain an estimation of the critical lateral-torsional buckling moment. It is pointed out that such a stepped beam finite element approach will exhibit a number of significant shortcomings as compared with a more detailed modeling approach. The most significant shortcoming is the fact that such an approach is unable to correctly duplicate the effect of the sloping flange bi-moment (a quantity frequently used to compute warping normal stresses in a cross section) on the buckling response.

SCOPE

The present research is aimed at studying the ultimate response of doubly symmetric, gently tapered I-shaped beams whose geometries are consistent with those commonly encountered in rafter sections used by the metal building industry in the U.S. A benchmark frame (see Figure 1) that is representative of a broad class of metal building designs is used as the basis for model construction in this present work. The study is analytical in nature; employing nonlinear finite element modeling techniques. The finite element techniques employed involve discretization of the member cross-section through the use of robust nonlinear shell finite elements located along the middle planes of the constituent plate components of the web-tapered member. Such an approach is not limited by the shortcomings in earlier finite element work on web-tapered beams, as discussed previously.

FINITE ELEMENT MODELING TECHNIQUES

Background

The commercial multipurpose finite element software package ABAQUS version 5.8-22 is employed in this research. All modeling reported herein considers both nonlinear geometric and material influences. The incremental solution strategy chosen for this work is a version of the

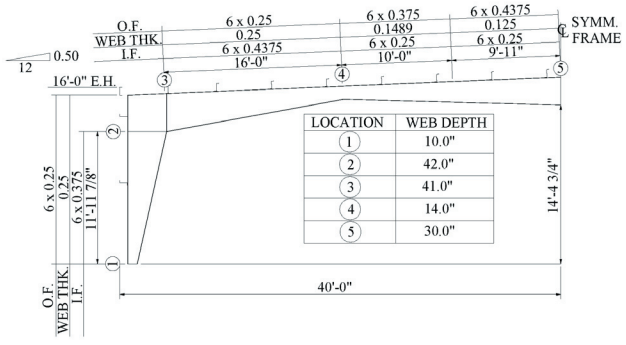

Fig. 1. Elevation view of benchmark frame.

Riks-Wempner method, modified as per Crisfield (1981) (ABAQUS 2003). The definition for rotation capacity adopted in the present discussion is that presented by ASCE (1971): $R = \{(\theta_u/\theta_p) - 1\}$, where θ_u is the rotation when the moment capacity drops below M_p on the unloading branch of the M-θ plot, and θ_p is the theoretical rotation at which the full plastic capacity is achieved based on elastic beam stiffness. This ductility response measure is described graphically in Figure 2 wherein θ_1 corresponds to θ_p, and θ_2 corresponds to θ_u in the ASCE definition. It is currently assumed that $R = 3$ is an adequate level of structural ductility to accommodate sufficient moment redistribution to allow formation of a collapse mechanism.

Material nonlinearity is modeled using ABAQUS' standard metal plasticity material model which is based on an incremental plasticity formulation employing associated flow assumptions in conjunction with a von Mises failure surface whose evolution in stress-space is governed by a simple isotropic hardening rule. In the present work, Grade 50 mild steel is considered; Figure 3 displays a schematic representation of the uniaxial material response that is consistent with what is used in the present work.

Modeling Overview

In modeling studies where inelastic buckling is investigated, it is important that the evolution of the modeling solution be carefully monitored so that any indication of bifurcation in the equilibrium path is carefully assessed in order to guarantee that the equilibrium branch being followed corresponds to the lowest energy state of the system (Earls and Shah, 2002). An imperfection seed is introduced into the finite element models to help ensure that the lowest energy equilibrium path is followed in the inelastic range. The imperfection shape employed in all models reported on herein is based on a linearized eigenvalue buckling analysis estimate of the first buckling mode; suitably scaled. The scaling factor employed in the imperfection used in the benchmark frame and verification study knee specimens of Sumner (1995) is $L_b/1000$; where L_b is the critical unbraced length. A scale factor of $L_b/500$ is used in the verification study with the beam of Prawel, Morrell, and Lee (1974), as well as the sub-assemblage beam used in the parametric study reported on herein. A scale factor of $L_b/500$ was suggested by Winter (1960) for use with bracing design formulae while the smaller $L_b/1000$ value is more consistent with fabrication tolerances for built-up members. A sensitivity study is performed on web-tapered beams with various imperfection scale factors and it is determined that the web-tapered beams themselves are quite insensitive to changes in the scale factor. The change in capacity of the beams is negligible between the scale factors of $L_b/1200$ and $L_b/100$. However, this is not the case for entire frameworks of such members. The frames examined were found to be sensitive to changes in the imperfection scale factor. Therefore, the normal out-of-straightness fabrication tolerance of $L_b/1000$ is utilized in the frame analysis work reported on in this paper.

A moment gradient is imposed across an unbraced length such that the theoretical plastic moment is attained at both ends of the beam, simultaneously. Parametric combinations of beam geometries modeled in ABAQUS include variations in slenderness ratios, h/t_w and $b_f/2t_f$, tapering angle γ, and beam unbraced length. The study includes flange widths of 6 in., 8 in., 10 in., and 12 in. and unbraced lengths of 60 in. and 75 in. Various plate thicknesses are employed as one means for varying plate slenderness ratios. The yield strength and modulus of elasticity of the steel used for the frame and subsequent parametric studies is 56.8 ksi and 29,600 ksi, respectively (see Figure 3). Two sections of the benchmark frame serve as the points of departure in the current parametric study; a section near the knee of the frame in the negative moment region, and a section near the ridge line in the positive moment region (see Figure 4). These portions of the benchmark frame's rafter sections, includ-

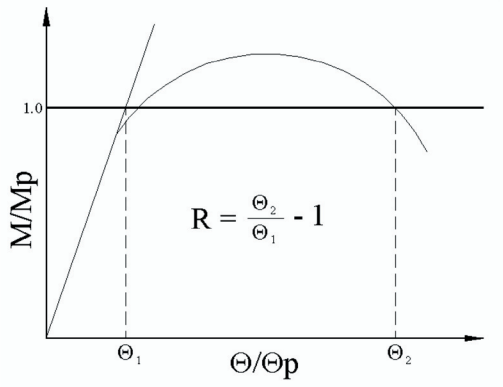

Fig. 2. Definition of rotation capacity.

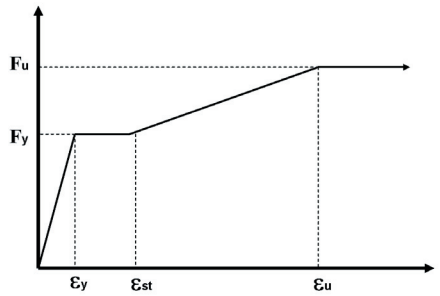

Material	F_y	F_u/F_y	$\varepsilon_{st}/\varepsilon_y$	$\varepsilon_u/\varepsilon_y$
Steel	56.8 ksi	1.34	13.6	30.4

Fig. 3. Uniaxial constitutive model considered (true stress vs. logarithmic strain).

ing the critical section determined by full-frame analysis, are modeled as simply supported beam sub-assemblages of the entire frame. The sections of the frame are modeled with an unbraced length, L_b, and an additional unbraced length, L_b, to either side of the critical section. The critical section retains the same material properties and geometry as in the frame. The additional lengths on either side of the critical section retains the same geometry as in the frame but the modulus of elasticity is increased by a factor of 10. By using a Young's Modulus of 290,000 ksi for the end sections, the material will approach a rigid condition and the additional beam lengths will force compatibility and continuity at the critical section junction. Utilizing the additional beam sections will allow point loads to be applied at the beam ends (Figure 5). This, in turn, allows for the applied moment at the beam end section to be exactly M_p. The unbraced lengths from the benchmark frame, L_b, are modeled in ABAQUS and later lengthened to $1.25L_b$ in order that an examination into the effects of beam unbraced length, on the behavior of web-tapered beams, might be made.

Instead of using the lateral bracing stiffnesses consistent with those of the benchmark frame model, idealized, rigid supports replace spring elements in order to prevent lateral movement at the brace points. This approach is adopted in order to limit the total number of parameters being studied in this work (in other words, the effects of bracing stiffness are not considered herein). Simple pinned-roller beam support conditions are imposed at the mid-height of the webs near the transition between flexible and rigid beam sections along the beam length (see Figure 5).

As a means of verifying the sub-assemblage model approach employed in the parametric study considered herein, a test model with geometry, bracing, and loading conditions identical to that of the benchmarks frame's critical section, is modeled in ABAQUS to assess the validity of the modeling techniques previously described. The critical section of the benchmark frame near the ridge-line (in other words, centerline of the frame) is identified from a consideration of the complete finite element model of the benchmark frame. The results of the sub-assemblage beam are very similar to the results for the critical section of the complete framework. The beam model fails at a load level that is 93 percent of the capacity exhibited in the full frame model. The modeled beam behavior is observed to be a close representation of the behavior of the same section in the benchmark frame. In fact, the modeled sub-assemblage beam is a slightly conservative representation of the critical benchmark frame since it fails at a lower load level than the frame.

Verification Study

When using the finite element method as the basis for a parametric study like that of the present work, it is desirable to validate the modeling strategies against previous experimental results directly related to the problem under investigation.

Beam Tests

One such experimental test that is considered suitable for a verification study related to the current research is the LB-3 beam tested by Prawel and others (1974). Planes of the shell element mesh surface used in the finite element analog of this specimen coincide with the middle surfaces of the constituent plate elements in the cross-section. Thus, the geometry of the experimental beam is directly incorporated into the nodal coordinates and shell thicknesses employed in the verification model. An appropriate constitutive relationship is constructed for the finite element model using the coupon test results reported on in the literature so as to be representative of the ASTM A242 grade of steel used in the experimental work.

The experimental beam tapers from a maximum depth of 16 in. to a minimum depth of 6 in. with an overall length of 144 in. The flanges are 4 in. wide and 0.25 in. thick and

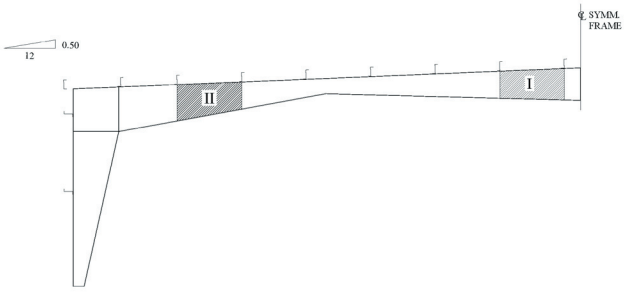

Fig. 4. Locations of modeled rafter sections in benchmark frame.

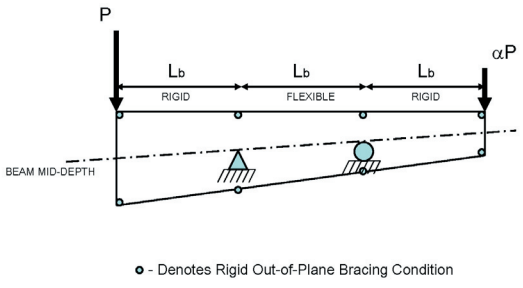

Fig. 5. Schematic representation of beam sub-assemblages.

the web is 0.105 in. thick. The values of $b_f/2t_f$ and h/t_w for this particular beam are higher than those permitted by the AISC LRFD Specification (AISC,1999) for plastic design of prismatic members. The beam is braced against lateral displacements at each of the stiffeners which are located at the ends of the beams and at the first and third quarter points; creating a maximum unbraced length of 72 in. Point loads are placed at the first and third quarter point stiffeners to create a moment gradient over the middle portion of the beam. Figure 6 depicts the overall geometry employed in the finite element model of the experimental beam. The magnitudes of the point loads are such that, in the elastic range, equal bending stresses exist over the entire center portion of the beam (Prawel and others, 1974). The beam is simply supported at the ends in a flexural, as well as torsional, sense.

In Prawel's experiment, the tapered beam reached a total load of 39.0 kips (P = 30.47 kips and βP = 8.53 kips) before unloading occurred. The maximum vertical deflection at the beam mid-span was reported by Prawel and others (1974) to be 1.04 in. Using an imperfection seed scale factor of $L_b/500$, in conjunction with an estimation of the first buckling mode (obtained from a linearized eigenvalue buckling analysis), the ABAQUS model reaches a total load of 36.07 kips (P = 28.18 kips and βP = 7.89 kips) before unloading occurs. A deflection at the finite element model beam mid-span of 0.903 in. is also recorded. Figure 7 displays a comparison of in-plane load versus mid-span deflection between the experimental and analytical beams. The results of the two beams are similar in that the two lines remain close to one another throughout the majority of the loading considered. The experimental beam tests by Prawel and others was not taken far enough into the unloading portion of the equilibrium path to be useful in comparing unloading characteristics between the actual beam and the ABAQUS model. Despite the fact that the ABAQUS model does not take into account residual stresses that were present in the LB-3 test beam, in an overall sense, the finite element model of the LB-3 beam captures the behavior of the experimental test results.

Sub-assemblage Tests

In addition to the previous beam study, two different geometries of rafter-to-column sub-assemblages (designated as KNEE 1 and 5 by Sumner (1995)) are modeled after the experimental tests carried out by Sumner and Murray at Virginia Tech. Figure 8 depicts the test setup used by Sumner and Murray and also gives the geometric data for each of the test specimens. Comparisons between the ABAQUS model response and the experimental results are presented in Figures 9 and 10. In the figure legends, the K percentages reference the bracing force used (in other words, the percentage of the force required to yield the compression flange) acting through a displacement of $L_b/1000$. Similarly, the I percentages represent the value of the scaling factor used in conjunction with the initial geometric imperfections obtained from a linearized eigenvalue buckling analysis.

Summary of Verification Results

Based on reasonably good agreement exhibited between finite element models of experimental test results related to web-tapered beams and web-tapered beam-to-rafter connections, it appears that the finite element modeling strategies adopted for use in the parametric beam study, to be reported on in the next section, seem adequate.

RESULTS AND DISCUSSION OF RESULTS

Parametric combinations of beam geometries modeled in ABAQUS include variations in slenderness ratios, h/t_w and

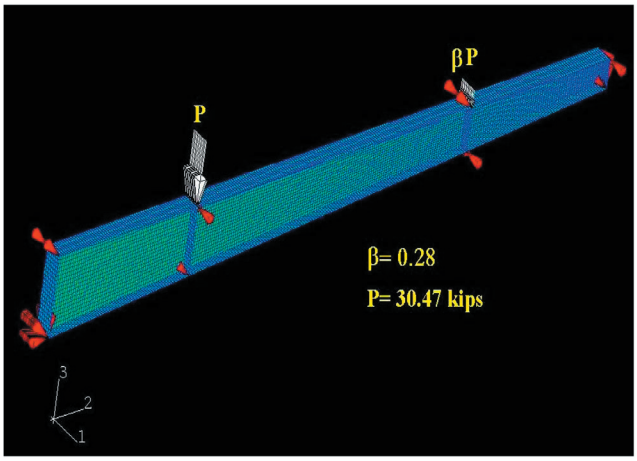

Fig. 6. Beam geometry from test of Prawel and others (1974).

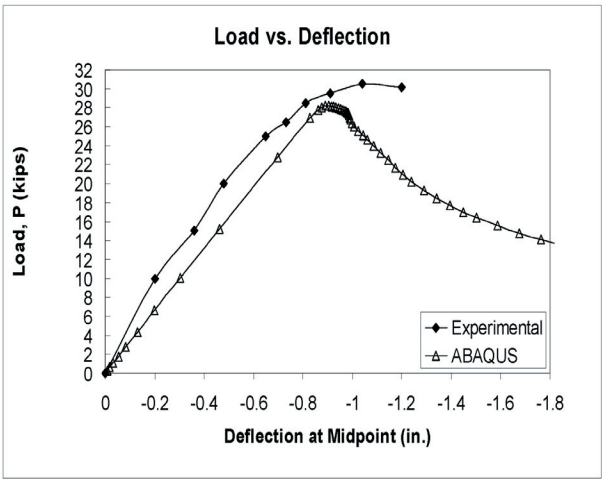

Fig. 7. Verification study results using the beam of Prawel and others (1974).

$b_f/2t_f$, tapering angle γ, and beam unbraced length; the flange widths considered include 6-in., 8-in., 10-in., and 12-in.-wide plates in addition to unbraced lengths of 60 in. and 75 in. Results from these parametric combinations are reported in Tables 1 through 4 (see Appendix).

Not surprisingly, it is observed from the present work that the behavior of web-tapered beams subjected to a moment gradient, equal to M_p at the beam ends, is similar to the behavior of prismatic beams subjected to a uniform moment within a given unbraced length. Beams with lower beam slenderness ratios (in other words, L_b/r_y) tend to fail in local buckling type modes while beams with higher beam slenderness ratios tend to fail in a lateral-torsional mode.

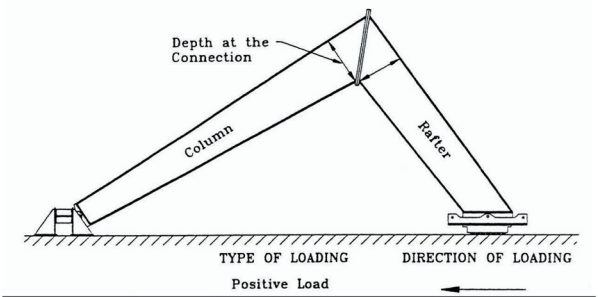

Test Designation	Depth at Connection (in.)	Flange Width (in.)	Column Web Thickness (in.)	Column Flange Thickness (in.)	Rafter Web Thickness (in.)	Rafter Flange Thickness (in.)
Knee 1	24	6	0.150	0.375	0.160	0.313
Knee 5	24	6	0.375	0.375	0.127	0.313

Fig. 8. Details on the experimental tests of Sumner (1995).

During the parametric study of the tapered beams whose unbraced length was 60 in., it is discovered that the beams with 6-in. flanges could only attain the theoretical cross-sectional plastic moment capacity, M_p, with compression flange slenderness, $b_f/2t_f$, values of 3.0 or less. However, beams with an 8-in. flange width could reach M_p at much higher (and more economical) slenderness ratios; $b_f/2t_f$ of approximately 6.4 or less. It is, however, noted that despite the short, unbraced lengths used (in other words, short compared with the AISC LRFD Specification L_p and L_{pd} limits), beams with 6-in. and 8-in.-wide flanges are observed to fail in a lateral-torsional buckling mode. It is additionally observed that this unexpected occurrence of lateral-torsional buckling is most prevalent in web-tapered beams whose cross-sectional plate slenderness values are somewhat lower than the compactness limit promulgated in the AISC LRFD Specification Table B5.1. Conversely, web-tapered beams with 10-in. and 12-in.-wide flanges, and reaching M_p with $b_f/2t_f$ ratios as high as 6.67 and 6.86, respectively, tended to fail due to local buckling; a condition becoming even more pronounced as sections become more and more noncompact according to AISC LRFD Specification Table B5.1. The foregoing behavior is best explained by the fact that local and global buckling effects are coupled in some way (in other words, flange and web local buckling interact in a very significant way in short web-tapered I-shaped rafter sections); these in turn interact with the global lateral-torsional mode.

It is surmised that the tendency for the web-tapered rafter geometries, having flange widths of 8 in., or less, to exhibit lateral-torsional buckling is a direct result of the lack of significant out-of-plane flexural rigidity provided by the narrow flanges (for example, the flanges behave as shallow

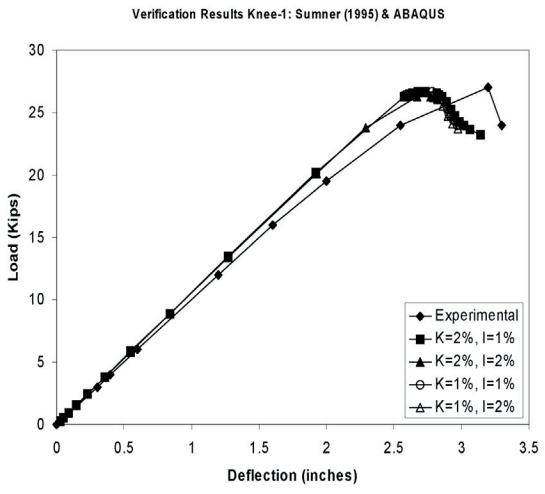

Fig. 9. Verification study results employing experimental results of Sumner (1995).

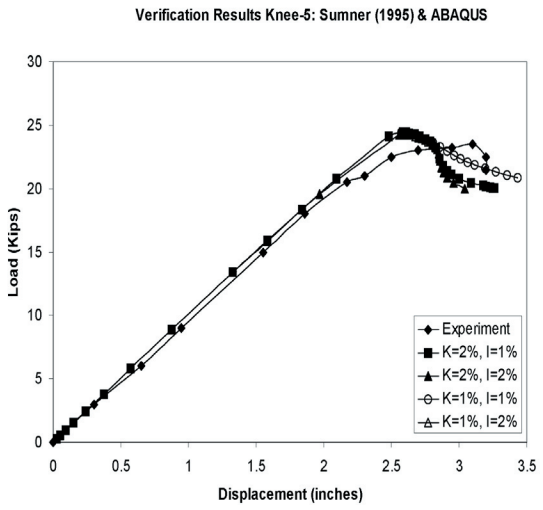

Fig. 10. Verification study results employing experimental results of Sumner (1995).

beams in resisting any tendency of the beam to move in the out-of-plane direction). In the case of the web-tapered beams having wider flanges, the flexural rigidity appears to be sufficient to resist the tendency that the beams have to exhibit out-of-plane deflection; thus the lateral-torsional deformation is sufficiently restrained to allow for the local buckling modes to be activated within the cross-sectional plate components.

When considering the effects of increasing the unbraced length, it is noted that the 75-in.-long beams exhibit lesser moment capacity as compared with shorter beams possessing the same cross-sectional slenderness ratios. In addition, the rotation capacity is also seen to decrease with increasing member length in identical cross-sections capable of reaching M_p.

The results from the beams that reach M_p are plotted in a three-dimensional design space; as described in detail elsewhere (Miller, 2003). As a simplification of this more complex treatment, the rotation capacity, R, can be plotted as a function of the plate slenderness ratios h/t_w and $b_f/2t_f$. Figures 11 and 12 present the h/t_w versus R and b_f/t_f versus R plots, respectively. The results presented in Figures 11 and 12 include both web-tapered rafter sections that are adequately braced (in other words, satisfying the AISC LRFD Specification's prismatic member bracing requirement, L_{pd}) as well those that are not so braced. The R value used in the plots is taken to be the average of the rotation capacity values calculated for the two ends of the web-tapered beams under consideration. In addition, the slenderness ratio, h/t_w, used in Figure 11 is the average value for the two ends of the beam.

One observation that can be made from Figures 11 and 12 is that current bracing requirements in the AISC LRFD Specification (AISC, 1999) are most likely not directly applicable to web-tapered beams of the geometries considered herein since beams having very similar cross-sections may achieve compact response whether or not the Specification's bracing requirements were satisfied. In other words, a web-tapered cross-section having a compact cross section according to Table B5.1 in the AISC LRFD Specification, as well as being adequately braced (vis-à-vis the L_{pd} requirement from Chapter F) might exhibit $R = 3$, or it might not. The point being that for web-tapered beams, it seems as though some fundamental differences in the underlying response are such that a different approach to specifying maximum unbraced lengths and compact cross-sections needs to be sought in future research.

Discussion of Results

Tables 1 through 4 present data and results from various parametric combinations of web-tapered beam geometries considered in the finite element modeling. From the data collected, it is observed that attainment of M_p is difficult to achieve in the case of a gradual moment gradient across the unbraced length so as to result in equal cross-sectional stresses in the end sections at ultimate. For the web-tapered I-shaped beam geometries considered, it is observed that an ultra-compact section ($\lambda_f << \lambda_p$, $\lambda_w << \lambda_p$) is needed in order to attain the plastic moment. While initially in the research this was viewed as a potential problem peculiar to web-tapered beams (in other words, web-tapered beams whose cross-sections easily satisfied prismatic member compact-

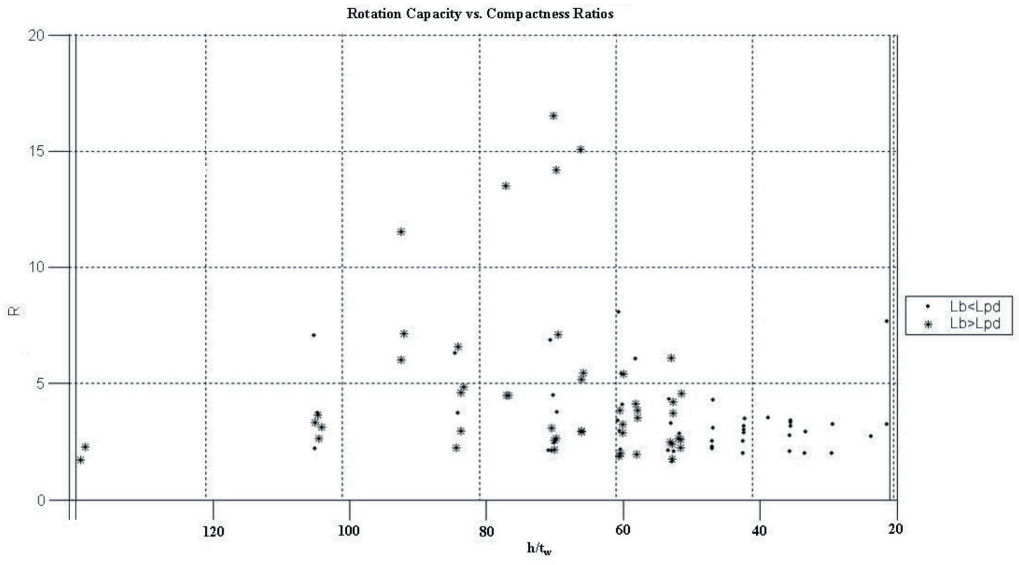

Fig. 11. Web slenderness ratio h/t_w *versus rotation capacity,* R.

ness criteria but that cannot attain M_p), it was later learned that prismatic beams suffer from a similar "short coming" under the action of a constant moment loading. Experimental results by Adams, Lay, and Galambos (1965) showed prismatic I-shaped beams loaded with a constant moment not reaching the plastic moment, M_p; despite the fact that the members easily satisfied the compactness requirements from Table B5.1 in the AISC LRFD Specification, while being adequately braced. Other experimental results that show similar difficulty of prismatic I-beams reaching the plastic moment, M_p, under uniform moment loadings include McDermott (1969) and Frost and Schilling (1964).

An interesting footnote to the results from the parametric study relates to the flatness of the overall moment-rotation response of the web-tapered members considered herein. It is noticed that if the geometry of a given beam is such that it could simultaneously attain the full plastic capacity at its ends then a rotation capacity of 3 is also observed to be easily attained.

The plastic design limit, L_{pd}, for doubly symmetric prismatic beams does not seem to be valid for doubly symmetric web-tapered I-shaped beams based on the three-dimensional R versus h/t_w and $b_f/2t_f$ plots described by Miller (2003). Modeled beams may, or may not, reach M_p, irrespective of satisfying the plastic design limit for prismatic beams, L_{pd}.

In addition, from the results presented in Tables 1 through 4, it appears that the AISC LRFD Specification Appendix F nominal moment strength equations accurately predict the moment capacity for beam geometries considered when the cross-sectional slenderness ratios remain close to the limiting cross-sectional plate slenderness values outlined in Table B5.1 of the AISC LRFD Specification. However, the design equations are conservative for sections that are very compact (in other words, the ratio of the ultimate moment capacity predicted by ABAQUS to the ultimate moment capacity predicted by the AISC LRFD Specification can be as high as 1.29) and unconservative for noncompact sections (in other words, the ratio of the ultimate moment capacity predicted by ABAQUS to the ultimate moment capacity predicted by the AISC LRFD Specification can be as low as 0.949).

CONCLUSIONS

Based on the present work, it appears that attainment of compact behavior in web-tapered beams subjected to a critical moment gradient, wherein the cross-sectional plastic capacity is developed simultaneously at both beam ends, is somewhat problematic when compactness is defined in a strict sense (in other words, $R = 3$). However, based on a survey of the literature related to the experimental testing of prismatic I-shaped beams subjected to a constant moment loading, it is observed that this is not a situation peculiar to web-tapered beams; prismatic beams experience very similar difficulties in attaining compact response despite being adequately braced and properly proportioned according to the Specification (AISC, 1999).

If a strict interpretation of compactness is nonetheless retained as the design basis, with its concomitant requirement for $R = 3$, then the current research indicates that economical plate slenderness ratios for the web-tapered beam flanges can only be achieved when flange plates possess widths of 8 in. or more. This recommendation stems from the fact that

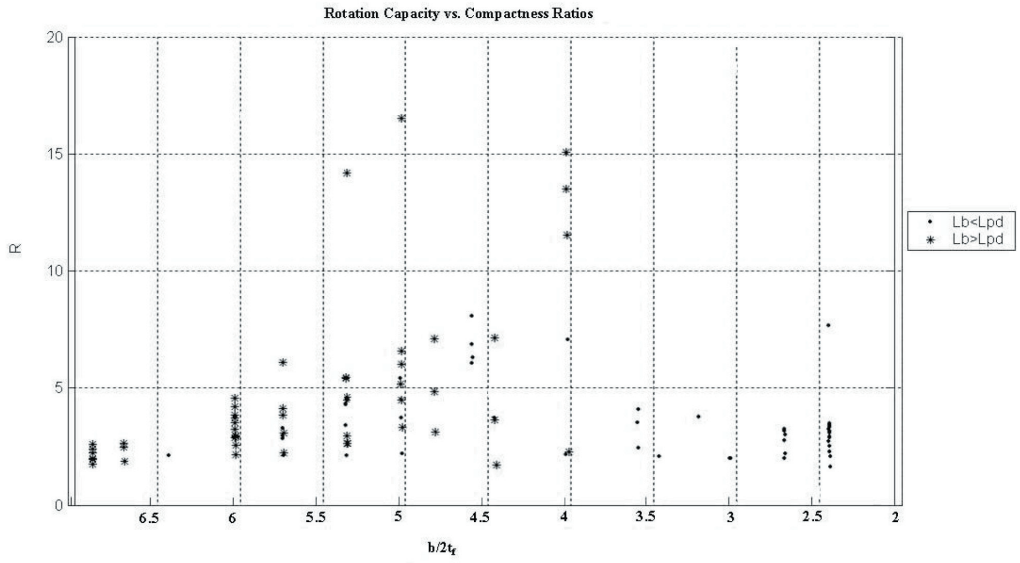

Fig. 12. Flange slenderness ratio $b_f/2t_f$ *versus rotation capacity,* R.

lateral-torsional type deformations are observed to occur in web-tapered rafter beams despite the fact that these examined rafter sections easily satisfy the unbraced length limits, L_p and L_{pd}, as outlined in Chapter F of the Specification. The results reported on herein (see Figures 11 and 12) indicate these same unbraced length limits are most likely not applicable for use with web-tapered I-shaped beams possessing geometries consistent with those considered herein.

Furthermore, it appears that the AISC LRFD Specification Appendix F nominal moment strength equations accurately predict the moment capacity in the beam geometries considered as long as the slenderness ratios remain close to the limiting cross-sectional plate slenderness values outlined in Table B5.1 of the Specification. However, these design equations are observed to be conservative for sections that are very compact and unconservative for noncompact cross-sectional proportions.

ACKNOWLEDGMENT

This research was partially funded by the Metal Building Manufacturers Association (MBMA). While the financial support of MBMA is acknowledged, it is pointed out that the observations and conclusions presented herein are solely those of the authors. The assistance of Gharib Ibrahim, in conducting the verification studies on the knee connections, is gratefully acknowledged.

NOTATION

b_f = Flange width, in.
d = Overall cross-sectional depth of beam, in.
t = Plate thickness, in.
t_f = Flange thickness, in.
t_w = Web thickness, in.
L_b = Unbraced length of web-tapered beam, in.
L_{pd} = Maximum unbraced length permitted for use with moment redistribution in prismatic members, in.
r_y = Weak axis radius of gyration for a cross-section, in.
λ_p = The maximum cross-sectional plate slenderness value permitted in cross sections of members that are to be used in applications where plastic moment redistribution is required
m(comp) = slope of compression flange relative to centroidal axis of the member
M(AISC) = Member moment capacity based on LRFD Appendix F, kip-in.
M_u(ABAQUS) = Member moment capacity as determined from nonlinear finite element analyses, kip-in.
α = Moment gradient factor defined as the moment at the larger end divided by the moment at the smaller end
β = Moment gradient factor defined by Prawel and others (1974) as the ratio of the load applied at the shallow beam end, to the load applied at the deep beam end
F_y = Steel yield stress, ksi
E = Modulus of elasticity, ksi
R = Cross-sectional rotation capacity

REFERENCES

ABAQUS (2003), *ABAQUS Theory Manual*, Hibbitt, Karlsson & Sorensen, Inc., Pawtucket, RI.

Adams, P.F., Lay, M.G., and Galambos, T.V. (1965), "Experiments on High Strength Steel Members," *WRC Bulletin, No. 110*, Welding Research Council, New York, NY, pp. 1-16.

ASCE (1971), *Plastic Design in Steel, A Guide and Commentary*, American Society of Civil Engineers, New York, New York, p. 80.

AISC (1999), *Load and Resistance Factor Design Specification for Structural Steel Buildings*, American Institute of Steel Construction Inc., Chicago, IL.

AISC (1989), *Specification for Structural Steel Buildings—Allowable Stress Design & Plastic Design*, American Institute of Steel Construction Inc., Chicago, IL.

Bazant, Z.P., and Cedolin, L. (1991), *Stability of Structures: Elastic, Inelastic, Fracture, and Damage Theories*, Oxford University Press, New York, NY.

Bleich, F. (1952), *Buckling Strength of Metal Structures*, McGraw-Hill Book Company, Inc., New York, NY.

Boley, B.A. (1963), "On the Accuracy of the Bernoulli-Euler Theory for Beams of Variable Section," *Journal of Applied Mechanics*, Vol. 30, pp. 373-378.

Crisfield, M.A. (1981), "A Fast Incremental/Iterative Solution Procedure that Handles 'Snap-Through'," *Computers & Structures*, Vol. 13, Pergamon Press Ltd., Great Britain, pp. 55-62.

Davis, B.D. (1996), *LRFD Evaluation of Full-Scale Metal Building Rigid Frame Tests*, masters thesis, Charles Via Department of Civil Engineering, Virginia Polytechnic Institute and State University, Blacksburg, VA.

Earls, C.J., and Shah, B.J. (2002), "High Performance Steel Bridge Girder Compactness," *Journal of Constructional Steel Research*, Elsevier Science Ltd., Great Britain, Vol. 58, pp. 859-880.

Frost, R.W., and Schilling, C.G. (1964), "Behavior of Hybrid Beams Subjected to Static Loads," *Journal of the Structural Division,* ASCE, Vol. 90, No. ST3, June, pp. 55-88.

Galambos, T.V. (1998), *Guide to Stability Design Criteria for Metal Structures*, Fifth Edition, John Wiley & Sons, Inc., New York, NY.

Haaijer, G., and Thurlimann, B. (1958), "On Inelastic Buckling in Steel," *Journal of the Engineering Mechanics Division*, Proceedings of the American Society of Civil Engineers, Paper 1581, EM 2, April, pp. 1581-1 to 1581-48.

Lee, G.C., Morrell, M.L., and Ketter, R.L. (1972), "Design of Tapered Members," *WRC Bulletin, No. 173*, Welding Research Council, New York, NY, June.

Lee, G.C., Ketter, R.L., and Hsu, T.L. (1981), *Design of Single Story Rigid Frames*, Metal Building Manufacturers Association, Cleveland, Ohio.

McDermott, J.F. (1969), "Plastic Bending of A514 Steel Beams," *Journal of the Structural Division*, ASCE, Vol. 95, No. ST9, September, pp. 1851-1871.

Miller, B.S. (2003), *Behavior of Web-Tapered Built-Up I-Shaped Beams*, masters thesis, Department of Civil and Environmental Engineering, University of Pittsburgh, Pittsburgh, PA. (Available on-line at http://etd.library.pitt.edu/ETD/available/etd-11132003-135449/)

Morrell, M.L., and Lee, G.C. (1974), "Allowable Stress for Web-Tapered Beams with Lateral Restraints," *WRC Bulletin, No. 192*, Welding Research Council, New York, NY, February.

Prawel, S.P., Morrell, M.L., and Lee, G.C. (1974), "Bending and Buckling Strength of Tapered Structural Members," *Welding Research Journal Supplement*, Vol. 53, February, pp. 75-84.

Sumner III, E.A. (1995), *Experimental and Analytical Investigation of the LRFD Strength of Tapered Members*, masters thesis, Charles Via Department of Civil Engineering, Virginia Polytechnic Institute and State University, Blacksburg, VA.

Teh, L.H., and Clarke, M.J. (1999), "Tracing Secondary Equilibrium Paths of Elastic Framed Structures," *Journal of Engineering Mechanics*, Vol. 125, No. 12, American Society of Civil Engineers, Reston Virginia, pp. 1358-1364.

Winter, G. (1960), "Lateral Bracing of Columns and Beams," *Transactions*, ASCE, Vol. 125, pp. 807-845.

APPENDIX

Table 1—Model 1. L_b = 60 in. Parametric Study Results

	E	F_y		End 1 = Shallow End			Web	Flanges								
	29600	56.8		End 2 = Deep End												
DESCRIPTION	t_f	b_f	t_w	d_w	$b_f/2t_f$	h/t_w	λ_p	λ_p	L_b/r_y	m(comp)	M(aisc)	M_u(abaqus)	M_u/M_p	M_u/M(aisc)	α	R
Model1 End 1	1.25	6	1.25	23.87	2.40	19.10	85.83	8.67	57.46	0.0417	17116.81	21647.25	1.0400	1.2647	1.2597	7.8654
Model1 End 2	1.25	6	1.25	27.89	2.40	22.31	85.83	8.67	60.20	0.0417	21230.99	27269.34	1.0400	1.2844		7.4881
Model1 End 1	1.25	6	0.75	23.995	2.40	31.99	85.83	8.67	52.37	0.0417	13497.76	15882.83	1.0100	1.1767	1.2396	3.3737
Model1 End 2	1.25	6	0.75	28.015	2.40	37.35	85.83	8.67	54.73	0.0417	16487.92	19688.48	1.0100	1.1941		3.2825
Model1 End 1	1.25	6	0.75	24.0575	2.40	32.08	85.83	8.67	53.25	0.0417	12934.35	15327.67	1.0100	1.1850	1.2430	3.4340
Model1 End 2	1.25	6	0.75	28.0775	2.40	37.44	85.83	8.67	55.69	0.0417	15841.15	19052.25	1.0100	1.2027		3.3487
Model1 End 1	1.25	6	0.625	23.87	2.40	38.19	85.83	8.67	48.66	0.0417	13913.38	15915.47	1.0100	1.1439	1.2259	3.5355
Model1 End 2	1.25	6	0.625	27.89	2.40	44.62	85.83	8.67	50.62	0.0417	16826.12	19510.25	1.0100	1.1595		3.4400
Model1 End 1	1.25	6	0.625	23.9325	2.40	38.29	85.83	8.67	49.31	0.0417	13390.01	15390.28	1.0100	1.1494	1.2282	3.2091
Model1 End 2	1.25	6	0.625	27.9525	2.40	44.72	85.83	8.67	51.34	0.0417	16220.91	18903.08	1.0100	1.1654		3.1356
Model1 End 1	1.25	6	0.625	23.995	2.40	38.39	85.83	8.67	50.03	0.0417	12841.10	14842.03	1.0100	1.1558	1.2312	2.9059
Model1 End 2	1.25	6	0.625	28.015	2.40	44.82	85.83	8.67	52.14	0.0417	15588.48	18272.86	1.0100	1.1722		2.8530
Model1 End 1	1.25	6	0.625	24.0575	2.40	38.49	85.83	8.67	50.81	0.0417	12264.65	14270.73	1.0100	1.1636	1.2347	2.5505
Model1 End 2	1.25	6	0.625	28.0775	2.40	44.92	85.83	8.67	53.01	0.0417	14926.87	17619.58	1.0100	1.1804		2.5146
Model1 End 1	1.25	6	0.5625	23.87	2.40	42.44	85.83	8.67	47.50	0.0417	13593.04	15404.74	1.0100	1.1333	1.2212	3.1182
Model1 End 2	1.25	6	0.5625	27.89	2.40	49.58	85.83	8.67	49.32	0.0417	16385.64	18813.00	1.0100	1.1481		3.0522
Model1 End 1	1.25	6	0.5625	23.9325	2.40	42.55	85.83	8.67	48.11	0.0417	13066.33	14875.43	1.0100	1.1385	1.2236	2.5551
Model1 End 2	1.25	6	0.5625	27.9525	2.40	49.69	85.83	8.67	50.00	0.0417	15776.53	18201.27	1.0100	1.1537		2.5130
Model1 End 1	1.25	6	0.5625	23.995	2.40	42.66	85.83	8.67	48.77	0.0417	12512.29	14178.42	1.0000	1.1332	1.2265	2.2801
Model1 End 2	1.25	6	0.5625	28.015	2.40	49.80	85.83	8.67	50.74	0.0417	15138.16	17389.71	1.0000	1.1487		2.2488
Model1 End 1	1.25	6	0.5	23.87	2.40	47.74	85.83	8.67	46.29	0.0417	13272.69	14746.54	1.0000	1.1110	1.2163	2.0711
Model1 End 2	1.25	6	0.5	27.89	2.40	55.78	85.83	8.67	47.97	0.0417	15945.15	17936.39	1.0000	1.1249		2.0404
Model1 End 1	1.25	6	0.5	23.995	2.40	47.99	85.83	8.67	47.46	0.0417	12183.07	13660.33	1.0000	1.1213	1.2215	1.6552
Model1 End 2	1.25	6	0.5	28.015	2.40	56.03	85.83	8.67	49.27	0.0417	14687.36	16686.07	1.0000	1.1361		1.6346
Model1 End 1	1.125	6	0.75	24.0575	2.67	32.08	85.83	8.67	53.25	0.0417	13025.41	15402.97	1.0100	1.1825	1.2418	3.1959
Model1 End 2	1.125	6	0.75	28.0775	2.67	37.44	85.83	8.67	55.69	0.0417	15937.41	19127.54	1.0100	1.2002		3.1295
Model1 End 1	1.125	6	0.75	24.12	2.67	32.16	85.83	8.67	54.22	0.0417	12484.98	14866.71	1.0100	1.1908	1.2451	2.7703
Model1 End 2	1.125	6	0.75	28.14	2.67	37.52	85.83	8.67	56.76	0.0417	15314.92	18510.21	1.0100	1.2086		2.7234
Model1 End 1	1.125	6	0.625	23.995	2.67	38.39	85.83	8.67	50.03	0.0417	12891.46	14888.29	1.0100	1.1549	1.2304	3.0198
Model1 End 2	1.125	6	0.625	28.015	2.67	44.82	85.83	8.67	52.14	0.0417	15642.19	18319.11	1.0100	1.1711		2.9756
Model1 End 1	1.125	6	0.5625	23.995	2.67	42.66	85.83	8.67	48.77	0.0417	12566.06	14229.89	1.0000	1.1324	1.2257	2.2084
Model1 End 2	1.125	6	0.5625	28.015	2.67	49.80	85.83	8.67	50.74	0.0417	15195.75	17441.19	1.0000	1.1478		2.1893
Model1 End 1	1	6	0.625	24.12	3.00	38.59	85.83	8.67	51.68	0.0417	11870.55	13724.14	1.0000	1.1562	1.2357	1.9989
Model1 End 2	1	6	0.625	28.14	3.00	45.02	85.83	8.67	53.97	0.0417	14459.20	16958.67	1.0000	1.1729		1.9879
Model1 End 1	1	6	0.5625	24.12	3.00	42.88	85.83	8.67	50.31	0.0417	11540.04	13194.61	0.9990	1.1434	1.2308	0
Model1 End 2	1	6	0.5625	28.14	3.00	50.03	85.83	8.67	52.45	0.0417	14006.76	16239.63	0.9990	1.1594		0
Model1 End 1	0.875	6	0.75	24.245	3.43	32.33	85.83	8.67	56.50	0.0417	11521.96	13751.07	1.0000	1.1935	1.2507	2.0826
Model1 End 2	0.875	6	0.75	28.265	3.43	37.69	85.83	8.67	59.26	0.0417	14194.10	17197.94	1.0000	1.2116		2.0702
Model1 End 1	1	8	0.25	24.12	4.00	96.48	85.83	8.67	30.48	0.0417	12742.61	13614.63	1.0100	1.0684	1.1908	7.8614
Model1 End 2	1	8	0.25	28.14	4.00	112.56	85.83	8.67	31.17	0.0417	15056.17	16212.84	1.0100	1.0768		6.2699
Model1 End 1	1.125	10	0.25	23.995	4.44	95.98	85.83	8.67	23.39	0.0417	17364.02	18457.54	1.0200	1.0630	1.1830	3.1946
Model1 End 2	1.125	10	0.25	28.015	4.44	112.06	85.83	8.67	23.80	0.0417	20415.46	21834.78	1.0200	1.0695		4.0552
Model1 End 1	0.875	8	0.4375	24.245	4.57	55.42	85.83	8.67	34.41	0.0417	12341.50	13912.33	1.0200	1.1273	1.2133	8.9029
Model1 End 2	0.875	8	0.4375	28.265	4.57	64.61	85.83	8.67	35.61	0.0417	14799.01	16880.28	1.0200	1.1406		7.2771
Model1 End 1	0.875	8	0.375	24.245	4.57	64.65	85.83	8.67	33.34	0.0417	12005.82	13249.03	1.0100	1.1036	1.2075	7.5913
Model1 End 2	0.875	8	0.375	28.265	4.57	75.37	85.83	8.67	34.41	0.0417	14340.52	15998.66	1.0100	1.1156		6.1609
Model1 End 1	0.875	8	0.3125	24.245	4.57	77.58	85.83	8.67	32.24	0.0417	11670.15	12722.12	1.0100	1.0901	1.2013	6.9402
Model1 End 2	0.875	8	0.3125	28.265	4.57	90.45	85.83	8.67	33.16	0.0417	13882.02	15282.54	1.0100	1.1009		5.6978
Model1 End 1	0.875	8	0.25	24.245	4.57	96.98	85.83	8.67	31.09	0.0417	11334.47	12062.40	0.9990	1.0642	1.1944	0
Model1 End 2	0.875	8	0.25	28.265	4.57	113.06	85.83	8.67	31.86	0.0417	13423.53	14407.77	0.9990	1.0733		0
Model1 End 1	1	10	0.4375	24.12	5.00	55.13	85.83	8.67	25.68	0.0417	16589.29	18418.91	1.0300	1.1103	1.2007	30.139
Model1 End 2	1	10	0.4375	28.14	5.00	64.32	85.83	8.67	26.40	0.0417	19725.09	22115.08	1.0300	1.1212		20.584
Model1 End 1	1	10	0.375	24.12	5.00	64.32	85.83	8.67	25.04	0.0417	16258.78	17887.09	1.0300	1.1001	1.1959	18.9
Model1 End 2	1	10	0.375	28.14	5.00	75.04	85.83	8.67	25.68	0.0417	19272.65	21391.22	1.0300	1.1099		14.135
Model1 End 1	1	10	0.3125	24.12	5.00	77.18	85.83	8.67	24.38	0.0417	15928.27	17186.78	1.0200	1.0790	1.1908	5.7369
Model1 End 2	1	10	0.3125	28.14	5.00	90.05	85.83	8.67	24.93	0.0417	18820.21	20466.70	1.0200	1.0875		7.4041
Model1 End 1	1	10	0.25	24.12	5.00	96.48	85.83	8.67	23.71	0.0417	15597.75	16496.79	1.0100	1.0576	1.1855	2.8281
Model1 End 2	1	10	0.25	28.14	5.00	112.56	85.83	8.67	24.16	0.0417	18367.77	19556.25	1.0100	1.0647		3.8104
Model1 End 1	0.75	8	0.5	24.37	5.33	48.74	85.83	8.67	36.81	0.0417	11290.62	12905.34	1.0100	1.1430	1.2251	4.7504
Model1 End 2	0.75	8	0.5	28.39	5.33	56.78	85.83	8.67	38.30	0.0417	13649.94	15809.99	1.0100	1.1582		3.8961
Model1 End 1	0.75	8	0.4375	24.37	5.33	55.70	85.83	8.67	35.66	0.0417	10949.72	12250.48	1.0000	1.1188	1.2194	3.7101
Model1 End 2	0.75	8	0.4375	28.39	5.33	64.89	85.83	8.67	37.01	0.0417	13185.34	14938.14	1.0000	1.1329		3.0947
Model1 End 1	1.125	12	0.375	23.995	5.33	63.99	85.83	8.67	20.00	0.0417	21227.30	22997.78	1.0300	1.0834	1.1879	13.701
Model1 End 2	1.125	12	0.375	28.015	5.33	74.71	85.83	8.67	20.41	0.0417	25034.27	27319.54	1.0300	1.0913		14.658
Model1 End 1	0.75	8	0.375	24.37	5.33	64.99	85.83	8.67	34.45	0.0417	10608.83	11723.40	1.0000	1.1051	1.2132	2.2748
Model1 End 2	0.75	8	0.375	28.39	5.33	75.71	85.83	8.67	35.66	0.0417	12720.73	14222.82	1.0000	1.1181		1.9569
Model1 End 1	1.125	12	0.3125	23.995	5.33	76.78	85.83	8.67	19.58	0.0417	20901.90	22253.29	1.0200	1.0647	1.1838	4.1328
Model1 End 2	1.125	12	0.3125	28.015	5.33	89.65	85.83	8.67	19.93	0.0417	24587.83	26343.83	1.0200	1.0714		5.0667
Model1 End 1	1.125	12	0.25	23.995	5.33	95.98	85.83	8.67	19.15	0.0417	20576.50	21519.02	1.0100	1.0458	1.1795	2.3850
Model1 End 2	1.125	12	0.25	28.015	5.33	112.06	85.83	8.67	19.44	0.0417	24141.40	25382.04	1.0100	1.0514		2.8718
Model1 End 1	0.875	10	0.5	24.245	5.71	48.49	85.83	8.67	27.02	0.0417	15175.12	17157.91	1.0300	1.1307	1.2099	6.7474
Model1 End 2	0.875	10	0.5	28.265	5.71	56.53	85.83	8.67	27.92	0.0417	18154.89	20759.49	1.0300	1.1435		5.4240
Model1 End 1	0.875	10	0.4375	24.245	5.71	55.42	85.83	8.67	26.33	0.0417	14839.44	16459.20	1.0200	1.1092	1.2051	3.5878
Model1 End 2	0.875	10	0.4375	28.265	5.71	64.61	85.83	8.67	27.13	0.0417	17696.40	19834.73	1.0200	1.1208		4.1198
Model1 End 1	0.875	10	0.375	24.245	5.71	64.65	85.83	8.67	25.61	0.0417	14503.76	15770.93	1.0100	1.0874	1.1999	2.8551
Model1 End 2	0.875	10	0.375	28.265	5.71	75.37	85.83	8.67	26.33	0.0417	17237.90	18924.14	1.0100	1.0978		3.2881
Model1 End 1	0.875	10	0.3125	24.245	5.71	77.58	85.83	8.67	24.88	0.0417	14168.08	15244.02	1.0100	1.0759	1.1944	2.0616
Model1 End 2	0.875	10	0.3125	28.265	5.71	90.45	85.83	8.67	25.49	0.0417	16779.41	18208.02	1.0100	1.0851		2.4032

Table 1—Model 1. (continued)
L_b = 60 in. Parametric Study Results

	E	F_y		End 1 = Shallow End			Web	Flanges								
	29600	56.8		End 2 = Deep End												
DESCRIPTION	t_f	b_f	t_w	d_w	$b_f/2t_f$	h/t_w	λ_p	λ_p	L_b/r_y	m(comp)	M(aisc)	M_u(abaqus)	M_u/M_p	M_u/M(aisc)	α	R
Model1 End 1	1	12	0.5	24.12	6.00	48.24	85.83	8.67	21.22	0.0417	19774.95	21889.96	1.0300	1.1070	1.1991	3.8657
Model1 End 2	1	12	0.5	28.14	6.00	56.28	85.83	8.67	21.80	0.0417	23489.13	26248.55	1.0300	1.1175		4.5342
Model1 End 1	0.5	6	0.5	24.62	6.00	49.24	85.83	8.67	60.09	0.0417	7092.99	8242.77	0.9602	1.1621	1.2569	0
Model1 End 2	0.5	6	0.5	28.64	6.00	57.28	85.83	8.67	63.23	0.0417	8781.84	10342.99	0.9586	1.1778		0
Model1 End 1	1	12	0.4375	24.12	6.00	55.13	85.83	8.67	20.78	0.0417	19444.43	21150.79	1.0200	1.0878	1.1951	3.0270
Model1 End 2	1	12	0.4375	28.14	6.00	64.32	85.83	8.67	21.30	0.0417	23036.69	25276.88	1.0200	1.0972		3.4602
Model1 End 1	0.5	6	0.4375	24.62	6.00	56.27	85.83	8.67	57.64	0.0417	6741.49	7675.76	0.9540	1.1386	1.2504	0
Model1 End 2	0.5	6	0.4375	28.64	6.00	65.46	85.83	8.67	60.54	0.0417	8304.85	9582.64	0.9524	1.1539		0
Model1 End 1	1	12	0.375	24.12	6.00	64.32	85.83	8.67	20.32	0.0417	19113.92	20624.14	1.0200	1.0790	1.1908	2.4101
Model1 End 2	1	12	0.375	28.14	6.00	75.04	85.83	8.67	20.78	0.0417	22584.25	24560.05	1.0200	1.0875		2.6792
Model1 End 1	0.5	6	0.375	24.62	6.00	65.65	85.83	8.67	55.03	0.0417	6390.00	7123.00	0.9487	1.1147	1.2431	0
Model1 End 2	0.5	6	0.375	28.64	6.00	76.37	85.83	8.67	57.66	0.0417	7827.87	8840.49	0.9472	1.1294		0
Model1 End 1	0.625	8	0.5	24.495	6.40	48.99	85.83	8.67	38.66	0.0417	9904.91	11394.12	1.0000	1.1503	1.2330	2.3045
Model1 End 2	0.625	8	0.5	28.515	6.40	57.03	85.83	8.67	40.35	0.0417	12043.18	14048.81	1.0000	1.1665		1.9463
Model1 End 1	0.625	8	0.4375	24.495	6.40	55.99	85.83	8.67	37.33	0.0417	9558.74	10807.30	0.9950	1.1306	1.2270	0
Model1 End 2	0.625	8	0.4375	28.515	6.40	65.18	85.83	8.67	38.88	0.0417	11572.41	13260.54	0.9950	1.1459		0
Model1 End 1	0.75	10	0.5	24.37	6.67	48.74	85.83	8.67	27.95	0.0417	13431.48	15216.14	1.0200	1.1329	1.2157	2.2891
Model1 End 2	0.75	10	0.5	28.39	6.67	56.78	85.83	8.67	28.96	0.0417	16133.22	18498.91	1.0200	1.1466		2.6967
Model1 End 1	0.75	10	0.4375	24.37	6.67	55.70	85.83	8.67	27.17	0.0417	13090.58	14534.61	1.0100	1.1103	1.2106	1.7374
Model1 End 2	0.75	10	0.4375	28.39	6.67	64.89	85.83	8.67	28.08	0.0417	15668.61	17595.07	1.0100	1.1230		1.9689
Model1 End 1	0.875	12	0.5	24.245	6.86	48.49	85.83	8.67	21.74	0.0417	17673.06	19538.19	1.0200	1.1055	1.2034	2.2617
Model1 End 2	0.875	12	0.5	28.265	6.86	56.53	85.83	8.67	22.39	0.0417	21052.28	23512.39	1.0200	1.1169		2.5222
Model1 End 1	0.875	12	0.4375	24.245	6.86	55.42	85.83	8.67	21.24	0.0417	17337.38	18819.73	1.0100	1.0855	1.1990	1.8895
Model1 End 2	0.875	12	0.4375	28.265	6.86	64.61	85.83	8.67	21.82	0.0417	20593.78	22565.75	1.0100	1.0958		2.0803
Model1 End 1	0.438	6	0.1875	24.6825	6.86	131.64	85.83	8.67	47.50	0.0417	4808.31	4975.63	0.9270	1.0348	1.2181	0
Model1 End 2	0.438	6	0.1875	28.7025	6.86	153.08	85.83	8.67	49.27	0.0417	5785.45	6060.94	0.9270	1.0476		0
Model1 End 1	0.5	8	0.3125	24.62	8.00	78.78	85.83	8.67	36.36	0.0417	7465.50	8027.56	0.9560	1.0753	1.2219	0
Model1 End 2	0.5	8	0.3125	28.64	8.00	91.65	85.83	8.67	37.79	0.0417	9006.19	9809.01	0.9560	1.0891		0
Model1 End 1	0.375	6	0.25	24.745	8.00	98.98	85.83	8.67	53.32	0.0417	4638.09	4872.57	0.9050	1.0506	1.2373	0
Model1 End 2	0.375	6	0.25	28.765	8.00	115.06	85.83	8.67	55.76	0.0417	5657.34	6028.61	0.9050	1.0656		0
Model1 End 1	0.375	6	0.1875	24.745	8.00	131.97	85.83	8.67	49.34	0.0417	4281.21	4356.56	0.9000	1.0176	1.2245	0
Model1 End 2	0.375	6	0.1875	28.765	8.00	153.41	85.83	8.67	51.33	0.0417	5174.08	5334.40	0.9000	1.0310		0
Model1 End 1	0.563	10	0.3125	24.5575	8.89	78.58	85.83	8.67	26.95	0.0417	9771.32	10273.89	0.9600	1.0514	1.2086	0
Model1 End 2	0.563	10	0.3125	28.5775	8.89	91.45	85.83	8.67	27.83	0.0417	11680.74	12416.85	0.9600	1.0630		0
Model1 End 1	0.438	8	0.25	24.6825	9.14	98.73	85.83	8.67	35.62	0.0417	6411.08	6619.86	0.9250	1.0326	1.2181	0
Model1 End 2	0.438	8	0.25	28.7025	9.14	114.81	85.83	8.67	36.95	0.0417	7713.93	8063.82	0.9250	1.0454		0
Model1 End 1	0.625	12	0.3125	24.495	9.60	78.38	85.83	8.67	21.28	0.0417	12434.18	12815.73	0.9590	1.0307	1.1989	0
Model1 End 2	0.625	12	0.3125	28.515	9.60	91.25	85.83	8.67	21.86	0.0417	14769.39	15364.90	0.9590	1.0403		0
Model1 End 1	0.313	6	0.25	24.8075	9.60	99.23	85.83	8.67	56.35	0.0417	4113.77	4247.63	0.8740	1.0325	1.2456	0
Model1 End 2	0.313	6	0.25	28.8275	9.60	115.31	85.83	8.67	59.11	0.0417	5049.20	5290.80	0.8740	1.0479		0
Model1 End 1	0.5	10	0.25	24.62	10.00	98.48	85.83	8.67	26.41	0.0417	8541.01	8645.17	0.9310	1.0122	1.2048	0
Model1 End 2	0.5	10	0.25	28.64	10.00	114.56	85.83	8.67	27.22	0.0417	10184.52	10415.70	0.9310	1.0227		0
Model1 End 1	0.5	10	0.1875	24.62	10.00	131.31	85.83	8.67	25.13	0.0417	8189.51	8109.34	0.9270	0.9902	1.1957	0
Model1 End 2	0.5	10	0.1875	28.64	10.00	152.75	85.83	8.67	25.77	0.0417	9707.53	9696.12	0.9270	0.9988		0
Model1 End 1	0.563	12	0.25	24.5575	10.67	98.23	85.83	8.67	20.89	0.0417	11027.93	11006.74	0.9350	0.9981	1.1953	0
Model1 End 2	0.563	12	0.25	28.5775	10.67	114.31	85.83	8.67	21.42	0.0417	13069.15	13156.82	0.9350	1.0067		0
Model1 End 1	0.375	8	0.25	24.745	10.67	98.98	85.83	8.67	37.01	0.0417	5708.28	5744.21	0.8900	1.0063	1.2245	0
Model1 End 2	0.375	8	0.25	28.765	10.67	115.06	85.83	8.67	38.50	0.0417	6898.77	7033.51	0.8900	1.0195		0
Model1 End 1	0.563	12	0.1875	24.5575	10.67	130.97	85.83	8.67	20.06	0.0417	10679.10	10472.59	0.9320	0.9807	1.1878	0
Model1 End 2	0.563	12	0.1875	28.5775	10.67	152.41	85.83	8.67	20.47	0.0417	12595.28	12439.10	0.9320	0.9876		0
Model1 End 1	0.375	8	0.1875	24.745	10.67	131.97	85.83	8.67	34.59	0.0417	5351.40	5248.73	0.8880	0.9808	1.2128	0
Model1 End 2	0.375	8	0.1875	28.765	10.67	153.41	85.83	8.67	35.79	0.0417	6415.51	6365.61	0.8880	0.9922		0
Model1 End 1	0.438	10	0.25	24.6825	11.43	98.73	85.83	8.67	27.14	0.0417	7659.67	7589.78	0.9030	0.9909	1.2095	0
Model1 End 2	0.438	10	0.25	28.7025	11.43	114.81	85.83	8.67	28.03	0.0417	9162.30	9179.81	0.9030	1.0019		0
Model1 End 1	0.5	12	0.25	24.62	12.00	98.48	85.83	8.67	21.30	0.0417	9968.01	9737.85	0.9090	0.9769	1.1988	0
Model1 End 2	0.5	12	0.25	28.64	12.00	114.56	85.83	8.67	21.88	0.0417	11839.83	11674.10	0.9090	0.9860		0

Table 2—Model 2.
L_b = 60 in. Parametric Study Results

	E	F_y		End 1 = Shallow End													
	29600	56.8		End 2 = Deep End			Web	Flanges									
DESCRIPTION	t_f	b_f	t_w	d_w	$b_f/2t_f$	h/t_w	λ_p	λ_p	L_b/r_y	m(comp)	M(aisc)	M_u(abaqus)	M_u/M_p	M_u/M(aisc)	α	R
Model2 End 1	1.25	6	0.875	24.2471	2.40	27.71	85.83	8.67	53.03	0.1823	15501.67	18166.69	1.0000	1.1719	1.5264	3.2310
Model2 End 2	1.25	6	0.875	32.6846	2.40	37.35	85.83	8.67	57.90	0.1823	22985.67	27729.56	1.0000	1.2064		2.5934
Model2 End 1	1.25	6	0.75	24.2471	2.40	32.33	85.83	8.67	51.04	0.1823	14840.07	17106.01	0.9990	1.1527	1.5087	0
Model2 End 2	1.25	6	0.75	32.6846	2.40	43.58	85.83	8.67	55.52	0.1823	21768.10	25807.52	0.9990	1.1856		0
Model2 End 1	1.25	6	0.625	24.2471	2.40	38.80	85.83	8.67	48.85	0.1823	14178.47	15967.01	0.9930	1.1261	1.4887	0
Model2 End 2	1.25	6	0.625	32.6846	2.40	52.30	85.83	8.67	52.85	0.1823	20550.53	23769.59	0.9930	1.1566		0
Model2 End 1	1.25	6	0.5625	24.2471	2.40	43.11	85.83	8.67	47.68	0.1823	13847.67	15417.77	0.9910	1.1134	1.4777	0
Model2 End 2	1.25	6	0.5625	32.6846	2.40	58.11	85.83	8.67	51.40	0.1823	19941.74	22782.15	0.9910	1.1424		0
Model2 End 1	1.25	6	0.5	24.2471	2.40	48.49	85.83	8.67	46.45	0.1823	13516.87	14840.54	0.9870	1.0979	1.4659	0
Model2 End 2	1.25	6	0.5	32.6846	2.40	65.37	85.83	8.67	49.89	0.1823	19332.96	21754.42	0.9870	1.1253		0
Model2 End 1	1.125	6	1	24.3721	2.67	24.37	85.83	8.67	56.62	0.1823	15157.01	18210.38	1.0000	1.2014	1.5539	3.6147
Model2 End 2	1.125	6	1	32.8096	2.67	32.81	85.83	8.67	62.10	0.1823	22868.04	28296.40	1.0000	1.2374		2.8871
Model2 End 1	1.125	6	0.875	24.3721	2.67	27.85	85.83	8.67	54.73	0.1823	14485.13	17156.03	1.0000	1.1844	1.5380	2.2109
Model2 End 2	1.125	6	0.875	32.8096	2.67	37.50	85.83	8.67	59.91	0.1823	21636.44	26385.66	1.0000	1.2195		1.7871
Model2 End 1	1.125	6	0.75	24.3721	2.67	32.50	85.83	8.67	52.60	0.1823	13813.24	16021.17	0.9950	1.1598	1.5200	0
Model2 End 2	1.125	6	0.75	32.8096	2.67	43.75	85.83	8.67	57.39	0.1823	20404.85	24352.55	0.9950	1.1935		0
Model2 End 1	1	6	1	24.4971	3.00	24.50	85.83	8.67	58.77	0.1823	14152.08	17210.94	1.0000	1.2161	1.5669	2.2013
Model2 End 2	1	6	1	32.9346	3.00	32.93	85.83	8.67	64.62	0.1823	21534.04	26967.48	1.0000	1.2523		1.7776
Model2 End 1	1	6	0.625	24.4971	3.00	39.20	85.83	8.67	51.90	0.1823	12105.25	13791.12	0.9840	1.1393	1.5120	0
Model2 End 2	1	6	0.625	32.9346	3.00	52.70	85.83	8.67	56.56	0.1823	17796.88	20852.45	0.9840	1.1717		0
Model2 End 1	1	8	0.4375	24.4971	4.00	55.99	85.83	8.67	33.54	0.1823	13979.79	15467.19	1.0100	1.1064	1.4469	16.6442
Model2 End 2	1	8	0.4375	32.9346	4.00	75.28	85.83	8.67	35.77	0.1823	19784.38	22380.09	1.0100	1.1312		13.5374
Model2 End 1	1	8	0.375	24.4971	4.00	65.33	85.83	8.67	32.58	0.1823	13638.65	14929.27	1.0100	1.0946	1.4339	14.7960
Model2 End 2	1	8	0.375	32.9346	4.00	87.83	85.83	8.67	34.55	0.1823	19161.52	21407.80	1.0100	1.1172		12.2230
Model2 End 1	1	8	0.3125	24.4971	4.00	78.39	85.83	8.67	31.58	0.1823	13297.51	14248.86	1.0000	1.0715	1.4200	12.5432
Model2 End 2	1	8	0.3125	32.9346	4.00	105.39	85.83	8.67	33.29	0.1823	18538.65	20233.18	1.0000	1.0914		10.5627
Model2 End 1	0.875	8	0.5	24.6221	4.57	49.24	85.83	8.67	35.56	0.1823	12912.72	14442.01	1.0000	1.1184	1.4716	6.8779
Model2 End 2	0.875	8	0.5	33.0596	4.57	66.12	85.83	8.67	38.28	0.1823	18535.23	21252.25	1.0000	1.1466		5.2298
Model2 End 1	0.875	8	0.4375	24.6221	4.57	56.28	85.83	8.67	34.52	0.1823	12566.34	13876.15	0.9980	1.1042	1.4587	0
Model2 End 2	0.875	8	0.4375	33.0596	4.57	75.56	85.83	8.67	36.99	0.1823	17905.25	20241.70	0.9980	1.1305		0
Model2 End 1	1	10	0.3125	24.4971	5.00	78.39	85.83	8.67	24.44	0.1823	16195.47	17145.33	1.0000	1.0586	1.4049	6.6935
Model2 End 2	1	10	0.3125	32.9346	5.00	105.39	85.83	8.67	25.57	0.1823	22394.74	24088.16	1.0000	1.0756		5.3727
Model2 End 1	1	10	0.25	24.4971	5.00	97.99	85.83	8.67	23.75	0.1823	15854.33	16579.51	0.9980	1.0457	1.3920	0
Model2 End 2	1	10	0.25	32.9346	5.00	131.74	85.83	8.67	24.69	0.1823	21771.88	23079.24	0.9980	1.0600		0
Model2 End 1	0.75	8	0.625	24.7471	5.33	39.60	85.83	8.67	39.15	0.1823	12208.81	14124.63	1.0000	1.1569	1.5107	4.9147
Model2 End 2	0.75	8	0.625	33.1846	5.33	53.10	85.83	8.67	42.69	0.1823	17938.33	21338.22	1.0000	1.1895		3.6651
Model2 End 1	0.75	8	0.4375	24.7471	5.33	56.56	85.83	8.67	35.78	0.1823	11153.74	12331.64	0.9870	1.1056	1.4732	0
Model2 End 2	0.75	8	0.4375	33.1846	5.33	75.85	85.83	8.67	38.55	0.1823	16026.87	18166.95	0.9870	1.1335		0
Model2 End 1	0.875	10	0.5	24.6221	5.71	49.24	85.83	8.67	27.10	0.1823	15448.13	17146.18	1.0100	1.1099	1.4506	4.4608
Model2 End 2	0.875	10	0.5	33.0596	5.71	66.12	85.83	8.67	28.95	0.1823	21909.08	24871.60	1.0100	1.1352		3.8172
Model2 End 1	1	12	0.5	24.4971	6.00	48.99	85.83	8.67	21.28	0.1823	20116.84	21855.99	1.0100	1.0865	1.4248	4.3118
Model2 End 2	1	12	0.5	32.9346	6.00	65.87	85.83	8.67	22.48	0.1823	28119.41	31139.42	1.0100	1.1074		3.3633
Model2 End 1	1	12	0.4375	24.4971	6.00	55.99	85.83	8.67	20.83	0.1823	19775.70	21318.06	1.0100	1.0780	1.4151	3.2228
Model2 End 2	1	12	0.4375	32.9346	6.00	75.28	85.83	8.67	21.90	0.1823	27496.55	30167.13	1.0100	1.0971		2.6819
Model2 End 1	1	12	0.25	24.4971	6.00	97.99	85.83	8.67	19.40	0.1823	18752.29	19333.62	0.9910	1.0310	1.3830	0
Model2 End 2	1	12	0.25	32.9346	6.00	131.74	85.83	8.67	20.07	0.1823	25627.96	26737.64	0.9910	1.0433		0
Model2 End 1	0.5	6	0.25	24.9971	6.00	99.99	85.83	8.67	49.45	0.1823	5795.09	6037.91	0.9200	1.0419	1.4858	0
Model2 End 2	0.5	6	0.25	33.4346	6.00	133.74	85.83	8.67	53.52	0.1823	8389.52	8970.83	0.9200	1.0693		0
Model2 End 1	0.625	8	0.1875	24.8721	6.40	132.65	85.83	8.67	31.46	0.1823	8313.76	8434.95	0.9490	1.0146	1.4167	0
Model2 End 2	0.625	8	0.1875	33.3096	6.40	177.65	85.83	8.67	33.11	0.1823	11571.66	11949.38	0.9490	1.0326		0
Model2 End 1	0.75	10	0.5625	24.7471	6.67	43.99	85.83	8.67	28.82	0.1823	14030.10	15753.46	1.0000	1.1228	1.4760	2.8064
Model2 End 2	0.75	10	0.5625	33.1846	6.67	58.99	85.83	8.67	31.08	0.1823	20192.88	23252.12	1.0000	1.1515		2.4318
Model2 End 1	0.75	10	0.5	24.7471	6.67	49.49	85.83	8.67	28.05	0.1823	13678.41	15179.52	0.9980	1.1097	1.4645	0
Model2 End 2	0.75	10	0.5	33.1846	6.67	66.37	85.83	8.67	30.12	0.1823	19555.72	22230.24	0.9980	1.1368		0
Model2 End 1	0.75	10	0.3125	24.7471	6.67	79.19	85.83	8.67	25.58	0.1823	12623.34	13267.05	0.9770	1.0510	1.4244	0
Model2 End 2	0.75	10	0.3125	33.1846	6.67	106.19	85.83	8.67	27.02	0.1823	17644.26	18897.91	0.9770	1.0711		0
Model2 End 1	0.875	12	0.5625	24.6221	6.86	43.77	85.83	8.67	22.30	0.1823	18329.92	20249.36	1.0100	1.1047	1.4449	2.9277
Model2 End 2	0.875	12	0.5625	33.0596	6.86	58.77	85.83	8.67	23.76	0.1823	25912.91	29258.12	1.0100	1.1291		2.2931
Model2 End 1	0.875	12	0.5	24.6221	6.86	49.24	85.83	8.67	21.80	0.1823	17983.54	19510.83	1.0000	1.0849	1.4350	2.1310
Model2 End 2	0.875	12	0.5	33.0596	6.86	66.12	85.83	8.67	23.14	0.1823	25282.93	27998.45	1.0000	1.1074		1.7929
Model2 End 1	0.875	12	0.3125	24.6221	6.86	78.79	85.83	8.67	20.24	0.1823	16944.38	17628.24	0.9850	1.0404	1.4019	0
Model2 End 2	0.875	12	0.3125	33.0596	6.86	105.79	85.83	8.67	21.15	0.1823	23392.98	24712.18	0.9850	1.0564		0
Model2 End 1	0.438	6	0.25	25.0596	6.86	100.24	85.83	8.67	51.25	0.1823	5262.72	5433.89	0.9010	1.0325	1.4994	0
Model2 End 2	0.438	6	0.25	33.4971	6.86	133.99	85.83	8.67	55.73	0.1823	7681.22	8147.69	0.9010	1.0607		0
Model2 End 1	0.563	8	0.1875	24.9346	7.11	132.98	85.83	8.67	32.02	0.1823	7597.35	7649.39	0.9360	1.0069	1.4242	0
Model2 End 2	0.563	8	0.1875	33.3721	7.11	177.98	85.83	8.67	33.82	0.1823	10618.52	10894.01	0.9360	1.0259		0
Model2 End 1	0.75	12	0.5625	24.7471	8.00	43.99	85.83	8.67	23.05	0.1823	16203.08	17818.26	0.9940	1.0997	1.4584	0
Model2 End 2	0.75	12	0.5625	33.1846	8.00	58.99	85.83	8.67	24.69	0.1823	23084.57	25986.48	0.9940	1.1257		0
Model2 End 1	0.75	12	0.5	24.7471	8.00	49.49	85.83	8.67	22.49	0.1823	15851.39	17173.70	0.9880	1.0834	1.4478	0
Model2 End 2	0.75	12	0.5	33.1846	8.00	66.37	85.83	8.67	23.99	0.1823	22447.42	24864.02	0.9880	1.1077		0
Model2 End 1	0.625	10	0.375	24.8721	8.00	66.33	85.83	8.67	27.45	0.1823	11195.56	11938.22	0.9670	1.0663	1.4544	0
Model2 End 2	0.625	10	0.375	33.3096	8.00	88.83	85.83	8.67	29.37	0.1823	15914.43	17362.51	0.9670	1.0910		0
Model2 End 1	0.75	12	0.3125	24.7471	8.00	79.19	85.83	8.67	20.71	0.1823	14796.32	15263.42	0.9690	1.0316	1.4115	0
Model2 End 2	0.75	12	0.3125	33.1846	8.00	106.19	85.83	8.67	21.74	0.1823	20535.96	21544.77	0.9690	1.0491		0
Model2 End 1	0.5	8	0.25	24.9971	8.00	99.99	85.83	8.67	34.66	0.1823	7243.51	7410.34	0.9250	1.0230	1.4578	0
Model2 End 2	0.5	8	0.25	33.4346	8.00	133.74	85.83	8.67	37.13	0.1823	10317.15	10802.51	0.9250	1.0470		0
Model2 End 1	0.5	8	0.1875	24.9971	8.00	133.32	85.83	8.67	32.71	0.1823	6881.05	6867.54	0.9210	0.9980	1.4331	0
Model2 End 2	0.5	8	0.1875	33.4346	8.00	178.32	85.83	8.67	34.69	0.1823	9665.49	9842.06	0.9210	1.0183		0

Table 2—Model 2. (continued)
L_b = 60 in. Parametric Study Results

	E	F_y		End 1 = Shallow End			Web	Flanges								
	29600	56.8		End 2 = Deep End												
DESCRIPTION	t_f	b_f	t_w	d_w	$b_f/2t_f$	h/t_w	λ_p	λ_p	L_b/r_y	m(comp)	M(aisc)	M_u(abaqus)	M_u/M_p	M_u/M(aisc)	α	R
Model2 End 1	0.563	10	0.375	24.9346	8.89	66.49	85.83	8.67	28.11	0.1823	10306.11	10930.03	0.9540	1.0605	1.4639	0
Model2 End 2	0.563	10	0.375	33.3721	8.89	88.99	85.83	8.67	30.18	0.1823	14731.19	16001.00	0.9540	1.0862		0
Model2 End 1	0.563	10	0.1875	24.9346	8.89	132.98	85.83	8.67	24.73	0.1823	9226.88	9144.98	0.9330	0.9911	1.4087	0
Model2 End 2	0.563	10	0.1875	33.3721	8.89	177.98	85.83	8.67	25.93	0.1823	12787.14	12882.23	0.9330	1.0074		0
Model2 End 1	0.438	8	0.1875	25.0596	9.14	133.65	85.83	8.67	33.58	0.1823	6164.87	6073.49	0.9010	0.9852	1.4440	0
Model2 End 2	0.438	8	0.1875	33.4971	9.14	178.65	85.83	8.67	35.78	0.1823	8712.54	8770.04	0.9010	1.0066		0
Model2 End 1	0.625	12	0.375	24.8721	9.60	66.33	85.83	8.67	22.05	0.1823	13006.21	13448.13	0.9500	1.0340	1.4386	0
Model2 End 2	0.625	12	0.375	33.3096	9.60	88.83	85.83	8.67	23.44	0.1823	18324.06	19346.16	0.9500	1.0558		0
Model2 End 1	0.5	10	0.25	24.9971	10.00	99.99	85.83	8.67	26.49	0.1823	8691.93	8655.36	0.9150	0.9958	1.4383	0
Model2 End 2	0.5	10	0.25	33.4346	10.00	133.74	85.83	8.67	28.15	0.1823	12244.77	12449.37	0.9150	1.0167		0
Model2 End 1	0.5	10	0.1875	24.9971	10.00	133.32	85.83	8.67	25.19	0.1823	8329.47	8156.85	0.9160	0.9793	1.4165	0
Model2 End 2	0.5	10	0.1875	33.4346	10.00	178.32	85.83	8.67	26.51	0.1823	11593.11	11554.21	0.9160	0.9966		0
Model2 End 1	0.563	12	0.3125	24.9346	10.67	79.79	85.83	8.67	21.75	0.1823	11575.89	11569.37	0.9230	0.9994	1.4322	0
Model2 End 2	0.563	12	0.3125	33.3721	10.67	106.79	85.83	8.67	23.05	0.1823	16251.79	16570.21	0.9230	1.0196		0
Model2 End 1	0.563	12	0.1875	24.9346	10.67	132.98	85.83	8.67	20.10	0.1823	10856.41	10390.74	0.9090	0.9571	1.3976	0
Model2 End 2	0.563	12	0.1875	33.3721	10.67	177.98	85.83	8.67	20.95	0.1823	14955.76	14521.95	0.9090	0.9710		0
Model2 End 1	0.5	12	0.25	24.9971	12.00	99.99	85.83	8.67	21.36	0.1823	10140.35	9740.53	0.8930	0.9606	1.4241	0
Model2 End 2	0.5	12	0.25	33.4346	12.00	133.74	85.83	8.67	22.56	0.1823	14172.40	13871.29	0.8930	0.9788		0

Table 3—Model 1.
L_b = 75 in. Parametric Study Results

	E	F_y		End 1 = Shallow End			Web	Flanges								
	29600	56.8		End 2 = Deep End												
DESCRIPTION	t_f	b_f	t_w	d_w	$b_f/2t_f$	h/t_w	λ_p	λ_p	L_b/r_y	m(comp)	M(aisc)	M_u(abaqus)	M_u/M_p	M_u/M(aisc)	α	R
Model1-ex End 1	1.25	6	1.25	23.87	2.40	19.10	85.83	8.67	71.83	0.0333	16450.81	21022.81	1.0100	1.2779	1.2597	3.1754
Model1-ex End 2	1.25	6	1.25	27.89	2.40	22.31	85.83	8.67	75.24	0.0333	20404.92	26482.72	1.0100	1.2979		3.3471
Model1-ex End 1	1.25	6	1.125	23.87	2.40	21.22	85.83	8.67	70.16	0.0333	15896.13	20199.37	1.0200	1.2707	1.2543	2.6569
Model1-ex End 2	1.25	6	1.125	27.89	2.40	24.79	85.83	8.67	73.48	0.0333	19633.66	25336.62	1.0200	1.2905		2.8109
Model1-ex End 1	1.25	6	0.625	23.87	2.40	38.19	85.83	8.67	60.83	0.0333	13669.32	15663.34	0.9940	1.1459	1.2259	0
Model1-ex End 2	1.25	6	0.625	27.89	2.40	44.62	85.83	8.67	63.27	0.0333	16530.97	19201.17	0.9940	1.1615		0
Model1-ex End 1	1.25	6	0.5625	23.87	2.40	42.44	85.83	8.67	59.38	0.0333	13388.25	15130.20	0.9920	1.1301	1.2212	0
Model1-ex End 2	1.25	6	0.5625	27.89	2.40	49.58	85.83	8.67	61.65	0.0333	16138.78	18477.72	0.9920	1.1449		0
Model1-ex End 1	1.125	6	0.625	23.995	2.67	38.39	85.83	8.67	62.54	0.0333	12597.71	14593.47	0.9900	1.1584	1.2304	0
Model1-ex End 2	1.125	6	0.625	28.015	2.67	44.82	85.83	8.67	65.17	0.0333	15285.75	17956.36	0.9900	1.1747		0
Model1-ex End 1	1.125	6	0.5625	23.995	2.67	42.66	85.83	8.67	60.97	0.0333	12315.92	14116.05	0.9920	1.1462	1.2257	0
Model1-ex End 2	1.125	6	0.5625	28.015	2.67	49.80	85.83	8.67	63.42	0.0333	14893.27	17301.66	0.9920	1.1617		0
Model1-ex End 1	1.25	8	0.375	23.87	3.20	63.65	85.83	8.67	39.05	0.0333	16201.99	17302.22	1.0000	1.0679	1.1960	3.8397
Model1-ex End 2	1.25	8	0.375	27.89	3.20	74.37	85.83	8.67	40.05	0.0333	19204.59	20693.58	1.0000	1.0775		3.6964
Model1-ex End 1	1.125	8	0.4375	23.995	3.56	54.85	85.83	8.67	40.83	0.0333	15127.74	16418.25	1.0000	1.0853	1.2043	4.2023
Model1-ex End 2	1.125	8	0.4375	28.015	3.56	64.03	85.83	8.67	42.06	0.0333	18028.82	19772.19	1.0000	1.0967		3.9581
Model1-ex End 1	1.125	8	0.375	23.995	3.56	63.99	85.83	8.67	39.75	0.0333	14802.34	15907.27	1.0000	1.0746	1.1992	2.4319
Model1-ex End 2	1.125	8	0.375	28.015	3.56	74.71	85.83	8.67	40.84	0.0333	17582.39	19075.64	1.0000	1.0849		2.4523
Model1-ex End 1	1	8	0.4375	24.12	4.00	55.13	85.83	8.67	41.80	0.0333	13734.15	15028.80	1.0000	1.0943	1.2084	2.1174
Model1-ex End 2	1	8	0.4375	28.14	4.00	64.32	85.83	8.67	43.15	0.0333	16413.49	18160.64	1.0000	1.1064		2.1628
Model1-ex End 1	1	8	0.25	24.12	4.00	96.48	85.83	8.67	38.10	0.0333	12742.61	13358.51	0.9910	1.0483	1.1908	0
Model1-ex End 2	1	8	0.25	28.14	4.00	112.56	85.83	8.67	38.96	0.0333	15056.17	15907.85	0.9910	1.0566		0
Model1-ex End 1	1.25	10	0.1875	23.87	4.00	127.31	85.83	8.67	28.21	0.0333	18810.95	19352.23	1.0000	1.0288	1.1761	2.3194
Model1-ex End 2	1.25	10	0.1875	27.89	4.00	148.75	85.83	8.67	28.57	0.0333	22023.55	22760.43	1.0000	1.0335		2.2074
Model1-ex End 1	1.125	10	0.25	23.995	4.44	95.98	85.83	8.67	29.24	0.0333	17364.02	18276.58	1.0100	1.0526	1.1830	3.8924
Model1-ex End 2	1.125	10	0.25	28.015	4.44	112.06	85.83	8.67	29.75	0.0333	20415.46	21620.71	1.0100	1.0590		3.5885
Model1-ex End 1	1.125	10	0.1875	23.995	4.44	127.97	85.83	8.67	28.46	0.0333	17038.62	17584.64	1.0000	1.0320	1.1777	1.7571
Model1-ex End 2	1.125	10	0.1875	28.015	4.44	149.41	85.83	8.67	28.85	0.0333	19969.02	20710.10	1.0000	1.0371		1.6561
Model1-ex End 1	0.875	8	0.4375	24.245	4.57	55.42	85.83	8.67	43.01	0.0333	12341.50	13584.99	0.9960	1.1008	1.2133	0
Model1-ex End 2	0.875	8	0.4375	28.265	4.57	64.61	85.83	8.67	44.51	0.0333	14799.01	16483.10	0.9960	1.1138		0
Model1-ex End 1	0.875	8	0.375	24.245	4.57	64.65	85.83	8.67	41.68	0.0333	12005.82	13012.91	0.9920	1.0839	1.2075	0
Model1-ex End 2	0.875	8	0.375	28.265	4.57	75.37	85.83	8.67	43.01	0.0333	14340.52	15713.54	0.9920	1.0957		0
Model1-ex End 1	0.875	8	0.3125	24.245	4.57	77.58	85.83	8.67	40.30	0.0333	11670.15	12457.61	0.9890	1.0675	1.2013	0
Model1-ex End 2	0.875	8	0.3125	28.265	4.57	90.45	85.83	8.67	41.45	0.0333	13882.02	14964.78	0.9890	1.0780		0
Model1-ex End 1	1.25	12	0.375	23.87	4.80	63.65	85.83	8.67	24.67	0.0333	23341.96	25169.39	1.0300	1.0783	1.1855	7.5762
Model1-ex End 2	1.25	12	0.375	27.89	4.80	74.37	85.83	8.67	25.14	0.0333	27485.43	29838.42	1.0300	1.0856		6.6175
Model1-ex End 1	1.25	12	0.3125	23.87	4.80	76.38	85.83	8.67	24.19	0.0333	23021.62	24409.24	1.0200	1.0603	1.1817	5.1872
Model1-ex End 2	1.25	12	0.3125	27.89	4.80	89.25	85.83	8.67	24.59	0.0333	27044.94	28844.58	1.0200	1.0665		4.5250
Model1-ex End 1	1.25	12	0.25	23.87	4.80	95.48	85.83	8.67	23.71	0.0333	22701.28	23659.20	1.0100	1.0422	1.1777	3.3584
Model1-ex End 2	1.25	12	0.25	27.89	4.80	111.56	85.83	8.67	24.03	0.0333	26604.46	27864.54	1.0100	1.0474		2.8948
Model1-ex End 1	1	10	0.4375	24.12	5.00	55.13	85.83	8.67	32.10	0.0333	16589.29	18240.08	1.0200	1.0995	1.2007	5.5453
Model1-ex End 2	1	10	0.4375	28.14	5.00	64.32	85.83	8.67	33.00	0.0333	19725.09	21900.37	1.0200	1.1103		5.2790
Model1-ex End 1	1	10	0.375	24.12	5.00	64.32	85.83	8.67	31.30	0.0333	16258.78	17539.77	1.0100	1.0788	1.1959	4.5812
Model1-ex End 2	1	10	0.375	28.14	5.00	75.04	85.83	8.67	32.10	0.0333	19272.65	20975.85	1.0100	1.0884		4.3887
Model1-ex End 1	1	10	0.3125	24.12	5.00	77.18	85.83	8.67	30.48	0.0333	15928.27	17018.28	1.0100	1.0684	1.1908	3.7859
Model1-ex End 2	1	10	0.3125	28.14	5.00	90.05	85.83	8.67	31.17	0.0333	18820.21	20266.05	1.0100	1.0768		3.6647
Model1-ex End 1	1	10	0.25	24.12	5.00	96.48	85.83	8.67	29.64	0.0333	15597.75	16333.46	1.0000	1.0472	1.1855	2.2029
Model1-ex End 2	1	10	0.25	28.14	5.00	112.56	85.83	8.67	30.20	0.0333	18367.77	19362.62	1.0000	1.0542		2.1780
Model1-ex End 1	1.125	12	0.4375	23.995	5.33	54.85	85.83	8.67	25.51	0.0333	21552.71	23295.70	1.0200	1.0809	1.1918	5.7141
Model1-ex End 2	1.125	12	0.4375	28.015	5.33	64.03	85.83	8.67	26.10	0.0333	25480.71	27764.78	1.0200	1.0896		5.0992
Model1-ex End 1	0.75	8	0.4375	24.37	5.33	55.70	85.83	8.67	44.57	0.0333	10949.72	12115.73	0.9890	1.1065	1.2194	0
Model1-ex End 2	0.75	8	0.4375	28.39	5.33	64.89	85.83	8.67	46.26	0.0333	13185.34	14773.82	0.9890	1.1205		0
Model1-ex End 1	1.125	12	0.375	23.995	5.33	63.99	85.83	8.67	25.00	0.0333	21227.30	22551.22	1.0100	1.0624	1.1879	2.3851
Model1-ex End 2	1.125	12	0.375	28.015	5.33	74.71	85.83	8.67	25.51	0.0333	25034.27	26789.06	1.0100	1.0701		2.8717
Model1-ex End 1	1.125	12	0.3125	23.995	5.33	76.78	85.83	8.67	24.47	0.0333	20901.90	22035.12	1.0100	1.0542	1.1838	3.1021
Model1-ex End 2	1.125	12	0.3125	28.015	5.33	89.65	85.83	8.67	24.91	0.0333	24587.83	26085.55	1.0100	1.0609		2.7893
Model1-ex End 1	0.875	10	0.5	24.245	5.71	48.49	85.83	8.67	33.77	0.0333	15175.12	16824.74	1.0100	1.1087	1.2099	3.5289
Model1-ex End 2	0.875	10	0.5	28.265	5.71	56.53	85.83	8.67	34.89	0.0333	18154.89	20356.39	1.0100	1.1213		3.0620
Model1-ex End 1	0.875	10	0.4375	24.245	5.71	55.42	85.83	8.67	32.91	0.0333	14839.44	16297.84	1.0100	1.0983	1.2051	2.9783
Model1-ex End 2	0.875	10	0.4375	28.265	5.71	64.61	85.83	8.67	33.92	0.0333	17696.40	19640.27	1.0100	1.1098		2.9345
Model1-ex End 1	0.875	10	0.375	24.245	5.71	64.65	85.83	8.67	32.01	0.0333	14503.76	15614.78	1.0000	1.0766	1.1999	2.1209
Model1-ex End 2	0.875	10	0.375	28.265	5.71	75.37	85.83	8.67	32.91	0.0333	17237.90	18736.78	1.0000	1.0870		2.1323
Model1-ex End 1	1	12	0.5	24.12	6.00	48.24	85.83	8.67	26.53	0.0333	19774.95	21677.44	1.0200	1.0962	1.1991	3.9110
Model1-ex End 2	1	12	0.5	28.14	6.00	56.28	85.83	8.67	27.25	0.0333	23489.13	25993.71	1.0200	1.1066		3.5599
Model1-ex End 1	1	12	0.4375	24.12	6.00	55.13	85.83	8.67	25.97	0.0333	19444.43	21150.79	1.0200	1.0878	1.1951	2.9808
Model1-ex End 2	1	12	0.4375	28.14	6.00	64.32	85.83	8.67	26.62	0.0333	23036.69	25276.88	1.0200	1.0972		2.7426
Model1-ex End 1	1	12	0.375	24.12	6.00	64.32	85.83	8.67	25.40	0.0333	19113.92	20421.94	1.0100	1.0684	1.1908	2.2152
Model1-ex End 2	1	12	0.375	28.14	6.00	75.04	85.83	8.67	25.97	0.0333	22584.25	24319.26	1.0100	1.0768		2.0798
Model1-ex End 1	0.875	12	0.5	24.245	6.86	48.49	85.83	8.67	27.18	0.0333	17673.06	19346.64	1.0100	1.0947	1.2034	1.8158
Model1-ex End 2	0.875	12	0.5	28.265	6.86	56.53	85.83	8.67	27.99	0.0333	21052.28	23281.87	1.0100	1.1059		1.7048
Model1-ex End 1	0.438	6	0.1875	24.6825	6.86	131.64	85.83	8.67	59.37	0.0333	4691.40	4938.06	0.9200	1.0526	1.2181	0
Model1-ex End 2	0.438	6	0.1875	28.7025	6.86	153.08	85.83	8.67	61.59	0.0333	5644.77	6015.17	0.9200	1.0656		0
Model1-ex End 1	0.5	8	0.3125	24.62	8.00	78.78	85.83	8.67	45.45	0.0333	7465.50	7935.19	0.9450	1.0629	1.2219	0
Model1-ex End 2	0.5	8	0.3125	28.64	8.00	91.65	85.83	8.67	47.23	0.0333	9006.19	9696.14	0.9450	1.0766		0
Model1-ex End 1	0.375	6	0.25	24.745	8.00	98.98	85.83	8.67	66.65	0.0333	4448.75	4834.88	0.8980	1.0868	1.2373	0
Model1-ex End 2	0.375	6	0.25	28.765	8.00	115.06	85.83	8.67	69.70	0.0333	5426.39	5981.98	0.8980	1.1024		0
Model1-ex End 1	0.375	6	0.1875	24.745	8.00	131.97	85.83	8.67	61.68	0.0333	4154.73	4342.04	0.8970	1.0451	1.2245	0
Model1-ex End 2	0.375	6	0.1875	28.765	8.00	153.41	85.83	8.67	64.17	0.0333	5021.22	5316.62	0.8970	1.0588		0

Table 3—Model 1. (continued)
L_b = 75 in. Parametric Study Results

	E	F_y		End 1 = Shallow End			Web	Flanges								
	29600	56.8		End 2 = Deep End												
DESCRIPTION	t_f	b_f	t_w	d_w	$b_f/2t_f$	h/t_w	λ_p	λ_p	L_b/r_y	m(comp)	M(aisc)	M_u(abaqus)	M_u/M_p	M_u/M(aisc)	α	R
Model1-ex End 1	0.563	10	0.3125	24.5575	8.89	78.58	85.83	8.67	33.69	0.0333	9771.32	10134.76	0.9470	1.0372	1.2086	0
Model1-ex End 2	0.563	10	0.3125	28.5775	8.89	91.45	85.83	8.67	34.78	0.0333	11680.74	12248.71	0.9470	1.0486		0
Model1-ex End 1	0.438	8	0.25	24.6825	9.14	98.73	85.83	8.67	44.53	0.0333	6411.08	6541.14	0.9140	1.0203	1.2181	0
Model1-ex End 2	0.438	8	0.25	28.7025	9.14	114.81	85.83	8.67	46.19	0.0333	7713.93	7967.92	0.9140	1.0329		0
Model1-ex End 1	0.625	12	0.3125	24.495	9.60	78.38	85.83	8.67	26.60	0.0333	12434.18	12655.37	0.9470	1.0178	1.1989	0
Model1-ex End 2	0.625	12	0.3125	28.515	9.60	91.25	85.83	8.67	27.33	0.0333	14769.39	15172.64	0.9470	1.0273		0
Model1-ex End 1	0.313	6	0.25	24.8075	9.60	99.23	85.83	8.67	70.44	0.0333	3906.36	4213.61	0.8670	1.0787	1.2456	0
Model1-ex End 2	0.313	6	0.25	28.8275	9.60	115.31	85.83	8.67	73.89	0.0333	4794.61	5248.43	0.8670	1.0947		0
Model1-ex End 1	0.5	10	0.25	24.62	10.00	98.48	85.83	8.67	33.02	0.0333	8541.01	8505.88	0.9160	0.9959	1.2048	0
Model1-ex End 2	0.5	10	0.25	28.64	10.00	114.56	85.83	8.67	34.03	0.0333	10184.52	10247.88	0.9160	1.0062		0
Model1-ex End 1	0.5	10	0.1875	24.62	10.00	131.31	85.83	8.67	31.41	0.0333	8189.51	8021.86	0.9170	0.9795	1.1957	0
Model1-ex End 2	0.5	10	0.1875	28.64	10.00	152.75	85.83	8.67	32.21	0.0333	9707.53	9591.52	0.9170	0.9880		0
Model1-ex End 1	0.563	12	0.25	24.5575	10.67	98.23	85.83	8.67	26.11	0.0333	11027.93	10841.93	0.9210	0.9831	1.1953	0
Model1-ex End 2	0.563	12	0.25	28.5775	10.67	114.31	85.83	8.67	26.77	0.0333	13069.15	12959.82	0.9210	0.9916		0
Model1-ex End 1	0.375	8	0.25	24.745	10.67	98.98	85.83	8.67	46.26	0.0333	5890.62	5686.12	0.8810	0.9653	1.2245	0
Model1-ex End 2	0.375	8	0.25	28.765	10.67	115.06	85.83	8.67	48.13	0.0333	7119.14	6962.38	0.8810	0.9780		0
Model1-ex End 1	0.563	12	0.1875	24.5575	10.67	130.97	85.83	8.67	25.07	0.0333	10679.10	10326.51	0.9190	0.9670	1.1878	0
Model1-ex End 2	0.563	12	0.1875	28.5775	10.67	152.41	85.83	8.67	25.59	0.0333	12595.28	12265.59	0.9190	0.9738		0
Model1-ex End 1	0.375	8	0.1875	24.745	10.67	131.97	85.83	8.67	43.24	0.0333	5351.40	5171.89	0.8750	0.9665	1.2128	0
Model1-ex End 2	0.375	8	0.1875	28.765	10.67	153.41	85.83	8.67	44.74	0.0333	6415.51	6272.42	0.8750	0.9777		0
Model1-ex End 1	0.438	10	0.25	24.6825	11.43	98.73	85.83	8.67	33.92	0.0333	7659.67	7480.51	0.8900	0.9766	1.2095	0
Model1-ex End 2	0.438	10	0.25	28.7025	11.43	114.81	85.83	8.67	35.04	0.0333	9162.30	9047.65	0.8900	0.9875		0
Model1-ex End 1	0.5	12	0.25	24.62	12.00	98.48	85.83	8.67	26.63	0.0333	9968.01	9598.59	0.8960	0.9629	1.1988	0
Model1-ex End 2	0.5	12	0.25	28.64	12.00	114.56	85.83	8.67	27.35	0.0333	11839.83	11507.15	0.8960	0.9719		0

Table 4—Model 2.
L_b = 75 in. Parametric Study Results

	E	F_y			End 1 = Shallow End		Web	Flanges								
	29600	56.8			End 2 = Deep End											
DESCRIPTION	t_f	b_f	t_w	d_w	$b_f/2t_f$	h/t_w	λ_p	λ_p	L_b/r_y	m(comp)	M(aisc)	M_u(abaqus)	M_u/M_p	M_u/M(aisc)	α	R
Model2-ex End 1	1.25	6	1.125	24.2471	2.40	21.55	85.83	8.67	70.48	0.1458	16283.93	20031.02	0.9890	1.2301	1.5563	0
Model2-ex End 2	1.25	6	1.125	32.6846	2.40	29.05	85.83	8.67	77.19	0.1458	24603.50	31175.22	0.9890	1.2671		0
Model2-ex End 1	1.125	8	0.75	24.3721	3.56	32.50	85.83	8.67	45.90	0.1458	17073.89	19360.21	1.0000	1.1339	1.4882	3.6140
Model2-ex End 2	1.125	8	0.75	32.8096	3.56	43.75	85.83	8.67	49.67	0.1458	24743.28	28811.77	1.0000	1.1644		3.4260
Model2-ex End 1	1.125	8	0.625	24.3721	3.56	39.00	85.83	8.67	44.01	0.1458	16402.00	18269.25	0.9980	1.1138	1.4695	0
Model2-ex End 2	1.125	8	0.625	32.8096	3.56	52.50	85.83	8.67	47.34	0.1458	23511.69	26847.24	0.9980	1.1419		0
Model2-ex End 1	1	8	0.625	24.4971	4.00	39.20	85.83	8.67	45.30	0.1458	15003.20	16793.46	0.9930	1.1193	1.4810	0
Model2-ex End 2	1	8	0.625	32.9346	4.00	52.70	85.83	8.67	48.92	0.1458	21652.96	24871.16	0.9930	1.1486		0
Model2-ex End 1	1	8	0.4375	24.4971	4.00	55.99	85.83	8.67	41.92	0.1458	13979.79	15084.34	0.9850	1.0790	1.4469	0
Model2-ex End 2	1	8	0.4375	32.9346	4.00	75.28	85.83	8.67	44.71	0.1458	19784.38	21826.13	0.9850	1.1032		0
Model2-ex End 1	1	8	0.375	24.4971	4.00	65.33	85.83	8.67	40.72	0.1458	13638.65	14515.39	0.9820	1.0643	1.4339	0
Model2-ex End 2	1	8	0.375	32.9346	4.00	87.83	85.83	8.67	43.19	0.1458	19161.52	20814.32	0.9820	1.0863		0
Model2-ex End 1	1.125	10	0.3125	24.3721	4.44	77.99	85.83	8.67	30.05	0.1458	17982.93	18928.52	1.0000	1.0526	1.3979	6.9061
Model2-ex End 2	1.125	10	0.3125	32.8096	4.44	104.99	85.83	8.67	31.34	0.1458	24771.14	26461.04	1.0000	1.0682		7.3674
Model2-ex End 1	1.125	10	0.25	24.3721	4.44	97.49	85.83	8.67	29.29	0.1458	17646.99	18309.34	0.9950	1.0375	1.3861	0
Model2-ex End 2	1.125	10	0.25	32.8096	4.44	131.24	85.83	8.67	30.35	0.1458	24155.34	25378.15	0.9950	1.0506		0
Model2-ex End 1	0.875	8	0.25	24.6221	4.57	98.49	85.83	8.67	38.96	0.1458	11527.17	11970.29	0.9740	1.0384	1.4136	0
Model2-ex End 2	0.875	8	0.25	33.0596	4.57	132.24	85.83	8.67	40.94	0.1458	16015.31	16920.64	0.9740	1.0565		0
Model2-ex End 1	0.625	6	0.3125	24.8721	4.80	79.59	85.83	8.67	61.70	0.1458	7076.81	7538.29	0.9220	1.0652	1.4863	0
Model2-ex End 2	0.625	6	0.3125	33.3096	4.80	106.59	85.83	8.67	66.79	0.1458	10247.51	11203.78	0.9220	1.0933		0
Model2-ex End 1	1	10	0.4375	24.4971	5.00	55.99	85.83	8.67	32.18	0.1458	16877.75	18210.52	1.0000	1.0790	1.4285	5.1532
Model2-ex End 2	1	10	0.4375	32.9346	5.00	75.28	85.83	8.67	34.05	0.1458	23640.46	26013.48	1.0000	1.1004		5.2063
Model2-ex End 1	1	10	0.375	24.4971	5.00	65.33	85.83	8.67	31.38	0.1458	16536.61	17677.93	1.0000	1.0690	1.4171	4.4096
Model2-ex End 2	1	10	0.375	32.9346	5.00	87.83	85.83	8.67	33.03	0.1458	23017.60	25050.82	1.0000	1.0883		4.5609
Model2-ex End 1	1	10	0.3125	24.4971	5.00	78.39	85.83	8.67	30.55	0.1458	16195.47	17076.75	0.9960	1.0544	1.4049	0
Model2-ex End 2	1	10	0.3125	32.9346	5.00	105.39	85.83	8.67	31.97	0.1458	22394.74	23991.80	0.9960	1.0713		0
Model2-ex End 1	1.125	12	0.4375	24.3721	5.33	55.71	85.83	8.67	25.56	0.1458	21915.46	23473.81	1.0100	1.0711	1.4073	5.2225
Model2-ex End 2	1.125	12	0.4375	32.8096	5.33	74.99	85.83	8.67	26.79	0.1458	30341.16	33035.71	1.0100	1.0888		5.6594
Model2-ex End 1	1.125	12	0.375	24.3721	5.33	64.99	85.83	8.67	25.04	0.1458	21579.52	22941.36	1.0100	1.0631	1.3979	4.2176
Model2-ex End 2	1.125	12	0.375	32.8096	5.33	87.49	85.83	8.67	26.12	0.1458	29725.36	32070.79	1.0100	1.0789		4.7234
Model2-ex End 1	0.875	10	0.5625	24.6221	5.71	43.77	85.83	8.67	34.73	0.1458	15794.52	17514.46	1.0000	1.1089	1.4614	2.8529
Model2-ex End 2	0.875	10	0.5625	33.0596	5.71	58.77	85.83	8.67	37.25	0.1458	22539.06	25595.33	1.0000	1.1356		2.8085
Model2-ex End 1	0.875	10	0.5	24.6221	5.71	49.24	85.83	8.67	33.88	0.1458	15448.13	16942.47	0.9980	1.0967	1.4506	0
Model2-ex End 2	0.875	10	0.5	33.0596	5.71	66.12	85.83	8.67	36.19	0.1458	21909.08	24576.10	0.9980	1.1217		0
Model2-ex End 1	0.875	10	0.3125	24.6221	5.71	78.79	85.83	8.67	31.17	0.1458	14408.97	15193.30	0.9890	1.0544	1.4136	0
Model2-ex End 2	0.875	10	0.3125	33.0596	5.71	105.79	85.83	8.67	32.75	0.1458	20019.14	21476.54	0.9890	1.0728		0
Model2-ex End 1	1	12	0.5625	24.4971	6.00	43.55	85.83	8.67	27.15	0.1458	20457.98	22393.91	1.0100	1.0946	1.4339	4.4626
Model2-ex End 2	1	12	0.5625	32.9346	6.00	58.55	85.83	8.67	28.80	0.1458	28742.27	32111.71	1.0100	1.1172		4.6650
Model2-ex End 1	1	12	0.5	24.4971	6.00	48.99	85.83	8.67	26.60	0.1458	20116.84	21855.99	1.0100	1.0865	1.4248	3.4583
Model2-ex End 2	1	12	0.5	32.9346	6.00	65.87	85.83	8.67	28.10	0.1458	28119.41	31139.42	1.0100	1.1074		3.5953
Model2-ex End 1	1	12	0.4375	24.4971	6.00	55.99	85.83	8.67	26.03	0.1458	19775.70	21318.06	1.0100	1.0780	1.4151	2.8870
Model2-ex End 2	1	12	0.4375	32.9346	6.00	75.28	85.83	8.67	27.38	0.1458	27496.55	30167.13	1.0100	1.0971		2.9810
Model2-ex End 1	0.5	6	0.375	24.9971	6.00	66.66	85.83	8.67	69.10	0.1458	6288.98	6920.20	0.9020	1.1004	1.5296	0
Model2-ex End 2	0.5	6	0.375	33.4346	6.00	89.16	85.83	8.67	75.80	0.1458	9349.41	10585.08	0.9020	1.1322		0
Model2-ex End 1	0.5	6	0.25	24.9971	6.00	99.99	85.83	8.67	61.81	0.1458	5678.51	5946.02	0.9060	1.0471	1.4858	0
Model2-ex End 2	0.5	6	0.25	33.4346	6.00	133.74	85.83	8.67	66.90	0.1458	8220.76	8834.32	0.9060	1.0746		0
Model2-ex End 1	0.5	6	0.1875	24.9971	6.00	133.32	85.83	8.67	57.77	0.1458	5364.94	5467.63	0.9100	1.0191	1.4578	0
Model2-ex End 2	0.5	6	0.1875	33.4346	6.00	178.32	85.83	8.67	61.89	0.1458	7641.44	7970.50	0.9100	1.0431		0
Model2-ex End 1	0.875	12	0.5625	24.6221	6.86	43.77	85.83	8.67	27.87	0.1458	18329.92	20048.87	1.0000	1.0938	1.4449	2.2471
Model2-ex End 2	0.875	12	0.5625	33.0596	6.86	58.77	85.83	8.67	29.70	0.1458	25912.91	28968.43	1.0000	1.1179		2.2419
Model2-ex End 1	0.438	6	0.375	25.0596	6.86	66.83	85.83	8.67	72.08	0.1458	5738.44	6366.76	0.8910	1.1095	1.5442	0
Model2-ex End 2	0.438	6	0.375	33.4971	6.86	89.33	85.83	8.67	79.39	0.1458	8609.81	9831.82	0.8910	1.1419		0
Model2-ex End 1	0.875	12	0.3125	24.6221	6.86	78.79	85.83	8.67	25.30	0.1458	16944.38	17592.45	0.9830	1.0382	1.4019	0
Model2-ex End 2	0.875	12	0.3125	33.0596	6.86	105.79	85.83	8.67	26.44	0.1458	23392.98	24662.00	0.9830	1.0542		0
Model2-ex End 1	0.438	6	0.3125	25.0596	6.86	80.19	85.83	8.67	68.21	0.1458	5438.44	5850.41	0.8880	1.0758	1.5237	0
Model2-ex End 2	0.438	6	0.3125	33.4971	6.86	107.19	85.83	8.67	74.72	0.1458	8055.91	8914.43	0.8880	1.1066		0
Model2-ex End 1	0.438	6	0.1875	25.0596	6.86	133.65	85.83	8.67	59.58	0.1458	4819.30	4882.47	0.8920	1.0131	1.4702	0
Model2-ex End 2	0.438	6	0.1875	33.4971	6.86	178.65	85.83	8.67	64.14	0.1458	6913.67	7178.03	0.8920	1.0382		0
Model2-ex End 1	0.5	8	0.3125	24.9971	8.00	79.99	85.83	8.67	45.62	0.1458	7605.96	7957.57	0.9290	1.0462	1.4792	0
Model2-ex End 2	0.5	8	0.3125	33.4346	8.00	106.99	85.83	8.67	49.27	0.1458	10968.81	11770.89	0.9290	1.0731		0
Model2-ex End 1	0.375	6	0.25	25.1221	8.00	100.49	85.83	8.67	66.94	0.1458	4583.59	4767.64	0.8670	1.0402	1.5157	0
Model2-ex End 2	0.375	6	0.25	33.5596	8.00	134.24	85.83	8.67	73.17	0.1458	6756.54	7226.46	0.8670	1.0696		0
Model2-ex End 1	0.5	8	0.1875	24.9971	8.00	133.32	85.83	8.67	40.89	0.1458	6881.05	6852.63	0.9190	0.9959	1.4331	0
Model2-ex End 2	0.5	8	0.1875	33.4346	8.00	178.32	85.83	8.67	43.36	0.1458	9665.49	9820.69	0.9190	1.0161		0
Model2-ex End 1	0.375	6	0.1875	25.1221	8.00	133.98	85.83	8.67	61.92	0.1458	4272.54	4272.14	0.8650	0.9999	1.4852	0
Model2-ex End 2	0.375	6	0.1875	33.5596	8.00	178.98	85.83	8.67	67.01	0.1458	6183.77	6345.18	0.8650	1.0261		0
Model2-ex End 1	0.563	10	0.1875	24.9346	8.89	132.98	85.83	8.67	30.91	0.1458	9226.88	9174.38	0.9360	0.9943	1.4087	0
Model2-ex End 2	0.563	10	0.1875	33.3721	8.89	177.98	85.83	8.67	32.41	0.1458	12787.14	12923.65	0.9360	1.0107		0
Model2-ex End 1	0.438	8	0.25	25.0596	9.14	100.24	85.83	8.67	44.69	0.1458	6530.05	6561.05	0.8990	1.0047	1.4702	0
Model2-ex End 2	0.438	8	0.25	33.4971	9.14	133.99	85.83	8.67	48.10	0.1458	9367.87	9645.82	0.8990	1.0297		0
Model2-ex End 1	0.438	8	0.1875	25.0596	9.14	133.65	85.83	8.67	41.98	0.1458	6164.87	6033.04	0.8950	0.9786	1.4440	0
Model2-ex End 2	0.438	8	0.1875	33.4971	9.14	178.65	85.83	8.67	44.72	0.1458	8712.54	8711.64	0.8950	0.9999		0
Model2-ex End 1	0.625	12	0.3125	24.8721	9.60	79.59	85.83	8.67	26.67	0.1458	12649.17	12749.66	0.9370	1.0079	1.4243	0
Model2-ex End 2	0.625	12	0.3125	33.3096	9.60	106.59	85.83	8.67	28.17	0.1458	17679.68	18158.76	0.9370	1.0271		0
Model2-ex End 1	0.5	10	0.3125	24.9971	10.00	79.99	85.83	8.67	34.66	0.1458	9054.38	9212.85	0.9200	1.0175	1.4578	0
Model2-ex End 2	0.5	10	0.3125	33.4346	10.00	106.99	85.83	8.67	37.13	0.1458	12896.44	13430.15	0.9200	1.0414		0
Model2-ex End 1	0.5	10	0.25	24.9971	10.00	99.99	85.83	8.67	33.11	0.1458	8691.93	8645.90	0.9140	0.9947	1.4383	0
Model2-ex End 2	0.5	10	0.25	33.4346	10.00	133.74	85.83	8.67	35.19	0.1458	12244.77	12435.77	0.9140	1.0156		0

Table 4—Model 2. (continued)
L_b = 75 in. Parametric Study Results

	E	F_y		End 1 = Shallow End			Web	Flanges								
	29600	56.8		End 2 = Deep End												
DESCRIPTION	t_f	b_f	t_w	d_w	$b_f/2t_f$	h/t_w	λ_p	λ_p	L_b/r_y	m(comp)	M(aisc)	M_u(abaqus)	M_u/M_p	M_u/M(aisc)	α	R
Model2-ex End 1	0.563	12	0.375	24.9346	10.67	66.49	85.83	8.67	28.16	0.1458	11935.64	12131.02	0.9270	1.0164	1.4474	0
Model2-ex End 2	0.563	12	0.375	33.3721	10.67	88.99	85.83	8.67	30.04	0.1458	16899.81	17842.39	0.9420	1.0558		0
Model2-ex End 1	0.375	8	0.25	25.1221	10.67	100.49	85.83	8.67	46.44	0.1458	5816.70	5702.77	0.8660	0.9804	1.4852	0
Model2-ex End 2	0.375	8	0.25	33.5596	10.67	134.24	85.83	8.67	50.26	0.1458	8418.69	8470.03	0.8660	1.0061		0
Model2-ex End 1	0.563	12	0.1875	24.9346	10.67	132.98	85.83	8.67	25.12	0.1458	10856.41	10447.89	0.9140	0.9624	1.3976	0
Model2-ex End 2	0.563	12	0.1875	33.3721	10.67	177.98	85.83	8.67	26.19	0.1458	14955.76	14601.83	0.9140	0.9763		0
Model2-ex End 1	0.375	8	0.1875	25.1221	10.67	133.98	85.83	8.67	43.38	0.1458	5448.78	5169.50	0.8580	0.9487	1.4574	0
Model2-ex End 2	0.375	8	0.1875	33.5596	10.67	178.98	85.83	8.67	46.47	0.1458	7759.69	7534.17	0.8580	0.9709		0
Model2-ex End 1	0.5	12	0.25	24.9971	12.00	99.99	85.83	8.67	26.70	0.1458	10140.35	9653.27	0.8850	0.9520	1.4241	0
Model2-ex End 2	0.5	12	0.25	33.4346	12.00	133.74	85.83	8.67	28.20	0.1458	14172.40	13747.02	0.8850	0.9700		0